

Paleocene Radiolarian Faunas in the Deep-Marine Sediments Near Zhongba County, southern Tibet

Authors: Li, Xin, Li, Yalin, Wang, Chengshan, and Matsuoka, Atsushi

Source: Paleontological Research, 22(1) : 37-56

Published By: The Palaeontological Society of Japan

URL: <https://doi.org/10.2517/2017PR009>

The BioOne Digital Library (<https://bioone.org/>) provides worldwide distribution for more than 580 journals and eBooks from BioOne's community of over 150 nonprofit societies, research institutions, and university presses in the biological, ecological, and environmental sciences. The BioOne Digital Library encompasses the flagship aggregation BioOne Complete (<https://bioone.org/subscribe>), the BioOne Complete Archive (<https://bioone.org/archive>), and the BioOne eBooks program offerings ESA eBook Collection (<https://bioone.org/esa-ebooks>) and CSIRO Publishing BioSelect Collection (<https://bioone.org/csiro-ebooks>).

Your use of this PDF, the BioOne Digital Library, and all posted and associated content indicates your acceptance of BioOne's Terms of Use, available at www.bioone.org/terms-of-use.

Usage of BioOne Digital Library content is strictly limited to personal, educational, and non-commercial use. Commercial inquiries or rights and permissions requests should be directed to the individual publisher as copyright holder.

BioOne is an innovative nonprofit that sees sustainable scholarly publishing as an inherently collaborative enterprise connecting authors, nonprofit publishers, academic institutions, research libraries, and research funders in the common goal of maximizing access to critical research.

Paleocene radiolarian faunas in the deep-marine sediments near Zhongba County, southern Tibet

XIN LI¹, YALIN LI², CHENGSHAN WANG² AND ATSUSHI MATSUOKA³

¹Nanjing Institute of Geology and Palaeontology, Chinese Academy of Sciences, Nanjing 210008, China (e-mail: lixindida@163.com)

²Department of Earth Science and Resources, China University of Geosciences, Beijing 100083, China

³Faculty of Science, Niigata University, Niigata 950-2181, Japan

Received October 24, 2016; Revised manuscript accepted April 2, 2017

Abstract. An upper Paleocene radiolarian-bearing succession (ZN1) located in the southern part of the north subzone of the Tethyan Himalaya is composed of siliceous siltstones and claystones. In this paper, 23 species belonging to 13 genera are reported. Three new species, *Lychnocanium? pyramis* Li and Matsuoka sp. nov., *Lychnocanium? stypticum* Li and Matsuoka sp. nov., and *Pterocyrtidium sinense* Li and Matsuoka sp. nov., are described. Radiolarian assemblages from this succession can be compared with the *Bekoma campechensis* Zone (RP6), indicating a time interval of 61.5–58.23 Ma, i.e., late Paleocene. The radiolarian assemblages from the Yamdrok mélange, the Zheba section, and the Jiazhu section indicate that they are of the same age as those from the Zhinadibu 1 section. The lack of calcareous and coarse-grained terrestrial materials in the ZN1 section proves that the strata of this section were deposited in a relatively deep marine environment below the calcium carbonate compensation depth (CCD) and more distal to the continents during the late Paleocene. Coeval deep-water sediments near Saga were accumulated near the CCD.

Key words: Indian passive margin, late Paleocene, new species, radiolarian assemblages, southern Tibet

Introduction

The Yarlung-Tsangpo Suture Zone (YTSZ) is the southernmost and youngest amongst the sutures which subdivide the Tibetan Plateau into five east–west trending blocks. The YTSZ marks where the Neo-Tethys was consumed as the Indian continent approached northward and finally collided with the Eurasian continent.

Methods such as tectonic deformation, paleomagnetism, and magmatic analyses have been applied in interpreting the initial contact between the Eurasian and Indian continents. However, the timing of the initial contact is still controversial and ranges from the Late Cretaceous (~70 Ma) to the early Oligocene (~34 Ma) (e.g. Beck *et al.*, 1995; Aitchison *et al.*, 2000, 2007; Yin and Harrison, 2000; Ding, 2003; Najman, 2006; Ali and Aitchison, 2008).

The Paleocene is the final stage of the subduction of the Neo-Tethyan oceanic lithosphere beneath the southern margin of the Lhasa terrane (Yin and Harrison, 2000; Ding, 2003). Radiolarian biostratigraphic studies on the Paleocene pelagic strata along the YTSZ will provide direct clues for the subduction and collision.

Reports on radiolarian-based upper Paleocene marine-sediment succession along the YTSZ are relatively scarce. Liu and Aitchison (2002) found a late Paleocene radiolarian fauna from the green mudstone matrix of the Yamdrok mélange (Loc. 1 in Figure 1). Ding (2003) reported Paleocene radiolarians from flysches near Saga (Loc. 2 in Figure 1). Hu *et al.* (2015) reported late Paleocene radiolarians and nanofossils from the same section as Ding (2003). An early Eocene radiolarian assemblage from a section near Saga was reported (Li *et al.*, 2007) (Loc. 3 in Figure 1). Liang *et al.* (2012) reported a late Paleocene radiolarian assemblage from the sedimentary mélange west of Zhongba County (Loc. 4 in Figure 1). The previous reports on radiolarian-bearing upper Paleocene strata along the YTSZ are isolated and scattered. Because the strata are seriously disrupted and diachronous spatially, the detailed distribution and extension of Paleocene deep-marine sediments along the YTSZ remain unclear.

Radiolarians have been widely reported from upper Paleocene and lower Eocene sedimentary strata. Upper Paleocene deep-sea sediment cores containing a continuous succession of well preserved radiolarians are

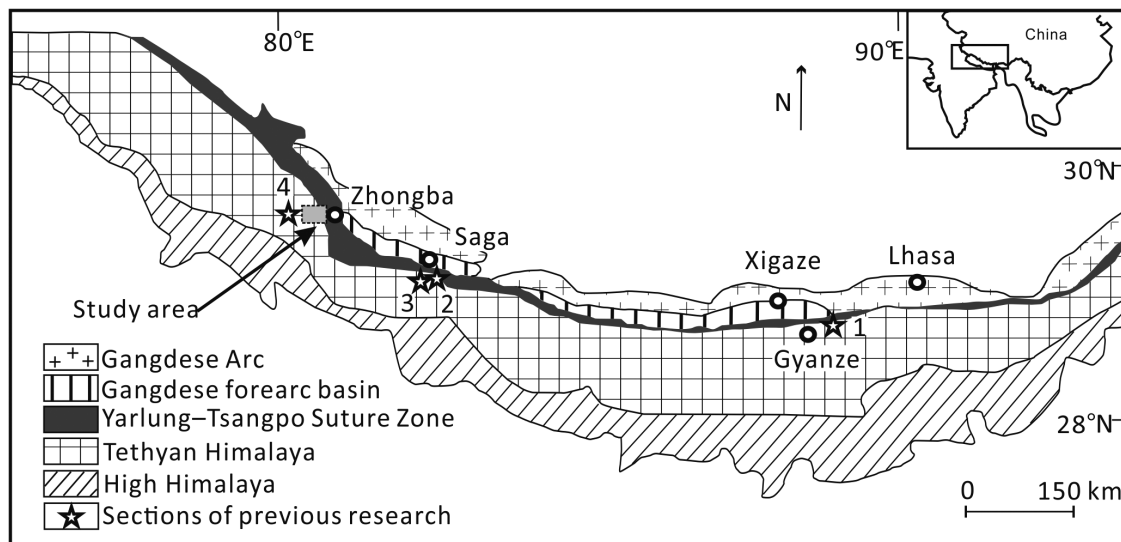


Figure 1. Geological map around the Yarlung-Tsangpo Suture Zone showing the major tectonic units (modified from Zhou *et al.*, 2007) and the locations of previous research: 1, Liu and Aitchison (2002); 2, Ding (2003) and Hu *et al.* (2015); 3, Li *et al.* (2007); 4, Liang *et al.* (2012).

known from Northwest Atlantic (Nishimura, 1987, 1992; Sanfilippo and Blome, 2001; Jackett *et al.*, 2008), Gulf of Mexico (Foreman, 1973; Sanfilippo and Riedel, 1973; Jackett *et al.*, 2008), Caribbean (Riedel and Sanfilippo, 1973), Northeast Atlantic (Liu *et al.*, 2011), Indian Ocean (Blome, 1992), South Pacific (Dumitrica, 1973; Hollis, 1993; O'Connor, 2001), and eastern New Zealand (O'Connor, 2001; Hollis, 2002). Sparse late Paleocene assemblages have been reported from land sections: Western Kuban in the former USSR (Borisenko, 1958), northern Cyprus (Sanfilippo *et al.*, 2003), southern Tibet (Liu and Aitchison, 2002; Ding, 2003; Li *et al.*, 2007; Liang *et al.*, 2012; Hu *et al.*, 2015), Japan (Nanayama, 1992; Oyaizu *et al.*, 2002), North America (Frizzell and Middour, 1951), western Cuba (Sanfilippo *et al.*, 1999), Canary Islands (Bustillo *et al.*, 1994), Southwest Pacific (Cluzel *et al.*, 2001), New Zealand (Hollis and Hanson, 1991; Hollis, 1993, 2006; Strong *et al.*, 1995), and South Africa (Jannou, 2007). Only samples from southern Tibet and New Zealand contain well preserved radiolarians. However, new species, which are abundant and typical in southern Tibet during the late Paleocene, have not been formally described.

In this paper, we present the results of a detailed study of upper Paleocene radiolarian biostratigraphy of a siliceous mudstone succession near Zhongba County and clarify the tectonic attributes of this succession. Three new species, *Lychnocanium? pyramis* Li and Matsuoka sp. nov., *Lychnocanium? stypticum* Li and Matsuoka sp. nov., and *Pterocyrtilidium sinense* Li and Matsuoka sp.

nov., are described. The age assignments of radiolarian assemblages are based on low-latitude zonation updated by Norris *et al.* (2014). We discuss the distribution of upper Paleocene radiolarian-bearing sediments and their depositional environments.

Geological setting

Four lithotectonic units are discriminated along the YTSZ from north to south: (1) Gangdese arc, (2) Gangdese forearc, (3) Yarlung-Tsangpo Suture Zone, and (4) Tethyan Himalaya (Figure 1). The Gangdese arc consists of Late Jurassic to early Paleogene granitoid intrusions (Debon *et al.*, 1986) and non-marine volcanic sequences of the Linzizong Formation of 68 to 43 Ma (Maluski *et al.*, 1982; Coulon *et al.*, 1986). The Gangdese forearc basin is located to the south of the Lhasa terrane. The forearc basin is occupied mostly by a sequence of Cretaceous to Paleogene turbiditic rocks (Einsele *et al.*, 1994). The YTSZ is characterized by a pile of ophiolitic bodies (e.g. Nicolas *et al.*, 1981; Aitchison and Davis, 2004).

The Tethyan Himalaya incorporates Mesozoic to lower Paleogene marine sequences deposited on the Indian passive continental margin. The strata have been roughly separated into two tectonic subzones by a line along the Gyirong-Kangmar Intracrustal Thrust, which was formed during the collision of the Indian and the Eurasian continents.

The northern subzone of the Tethyan Himalaya (NTH) consists of sandstones, siltstones, and limestones (Liu

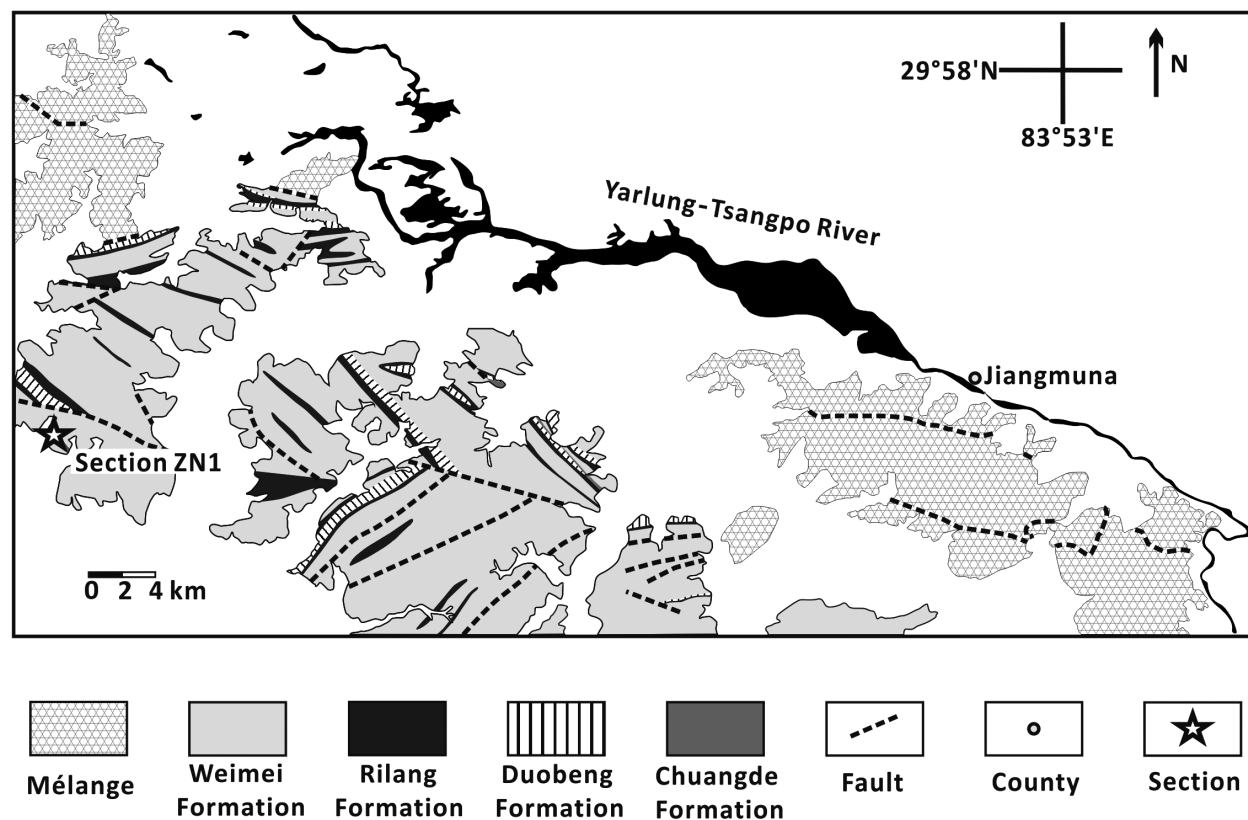


Figure 2. Strata distribution and the location of the ZN1 section in our research area (after 1:50,000 geological mapping investigations).

and Einsele, 1994; Hu *et al.*, 2008). Jurassic to lower Paleogene strata of the northern subzone exposed in the Gyangze area are relatively well studied and divided into five formations (Liu and Einsele, 1994; Li *et al.*, 1999; Wang *et al.*, 2000; Liu and Aitchison, 2002; Hu *et al.*, 2008): the Weimei Formation (Upper Jurassic quartz sandstones), the Rilang Formation (Lower Cretaceous volcanoclastic litharenites intercalated with siltstones), the Gyabula Formation (Lower to Upper Cretaceous black siltstones with pyrite nodules intercalated with sandstones), the Chuangde Formation (Upper Cretaceous violet-red limestones intercalated with thin marlstone beds), and the overlying Zongzhuo Formation (Upper Cretaceous to Paleocene dark gray to black shales enclosing various olistoliths of sandstones, limestones, and bedded cherts).

The southern subzone of the Tethyan Himalaya (STH) is composed mainly of carbonate and clastic sediments (Wan *et al.*, 2000). Well studied sections are located in the Gamba-Tingri area where the youngest shallow marine strata of the middle Eocene (Lutetian) have been reported (Wen, 1987; Willems *et al.*, 1996; Xu, 2000).

Material and methods

In our research area near Zhongba County, a previous 1:250,000 geological map defined the strata south of the Yarlung-Tsangpo River as the Upper Cretaceous to middle Eocene Sangdanlin Formation, Denggang Formation, Guoyala Formation, and Yanduo Formation (Institute of Geological Survey of Hebei Province, 2006). According to our field investigations from 2010 to 2013, the strata are divided into mélange and sedimentary strata. The sedimentary strata are located to the south of the mélange (Figure 2).

The sedimentary strata consist of quartz sandstones, lithic sandstones, siliceous mudstones interbedded with claystones, and limestones. The strata trend NW–SE and dip to the north or south. These strata are comparable with the strata exposed in the Gyanze area and subdivided into the Weimei Formation, the Rilang Formation, the Duobeng Formation, the Chuangde Formation, and the Denggang Formation (Du *et al.*, 2015).

The ZN1 (Zhinadibu 1) section (29°46'33"N, 83°16'40"E) is located in the southern part of the Mesozoic to Paleogene sedimentary strata (Figure 2). It is a succession of red

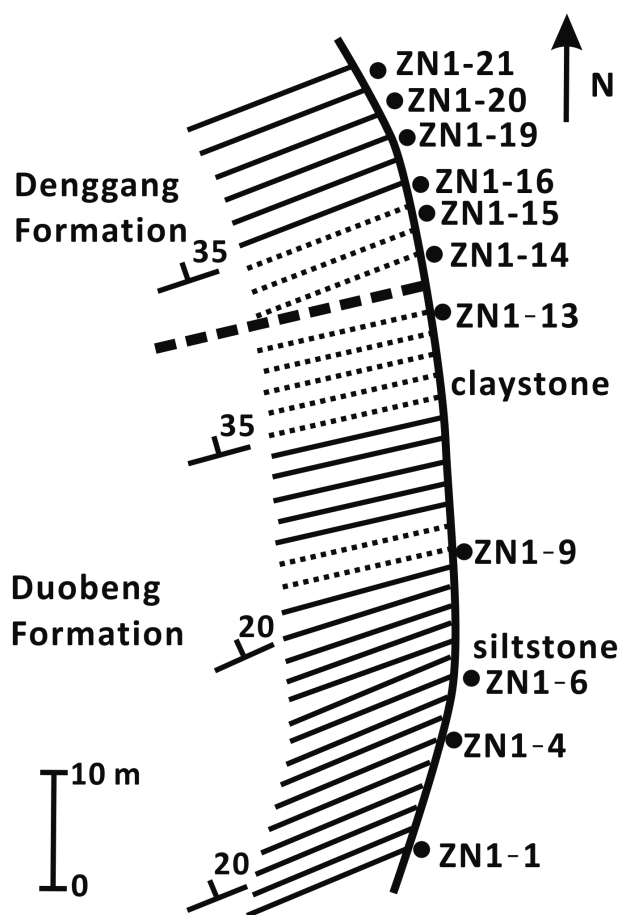


Figure 3. Route map showing the occurrence of the strata.

siliceous siltstone and grayish-green claystone (Figures 3, 4). The strata trend NW–SE and dip to the northeast. The strata of the section measured in this paper display a continuous, northeast-dipping succession. Laminations are visible in radiolarian-bearing beds. However, no sedimentary structures indicative of younging direction were observed. Twenty-one samples were collected from the 70 m-thick section. An inferred fault is located between ZN1-13 and ZN1-14.

Rock samples were disaggregated by leaching in 4% hydrofluoric acid for 20–24 hours. Samples were sieved and the >74 μm fraction was examined. Light microscope, stereoscopic microscope, and scanning electron microscope were used for observation, picking up, and identification of radiolarians. Of the 21 samples, six (ZN1-4, ZN1-6, ZN1-15, ZN1-16, ZN1-20, and ZN1-21) contain moderately to well preserved radiolarians. The fossil specimens reported in this paper are deposited in the Department of Geology, Niigata University.

Radiolarian assemblages and age assignments

Of the six samples, which contain moderately to well preserved radiolarians, two (ZN1-4 and ZN1-6) contain a radiolarian assemblage which is comparable with the *Costata* Subzone of the *Turbocapsula* Zone (O’Dogherty, 1994), indicating an Early Cretaceous (Aptian) age. Radiolarian assemblages from Lower Cretaceous strata in our research area have been reported by Li *et al.* (2017). The other four samples (ZN1-15, ZN1-16, ZN1-20, and ZN1-21) yield late Paleocene radiolarian assemblages (Figure 4).

Radiolarian zonal schemes for the Paleocene and lower Eocene are summarized below (Figure 5). Foreman (1973) defined four radiolarian zones for the uppermost Paleocene to lower-middle Eocene based on samples from the Gulf of Mexico: the *Bekoma bidartensis* Zone, the *Buryella clinata* Zone, the *Phormocyrtis striata striata* Zone, and the *Theocotyle cryptocephala* Zone (from the oldest to youngest). The stratigraphic interval, which is lower than the *Bekoma bidartensis* Zone, was expressed as “unzoned interval”. Nishimura (1987, 1992) defined this interval as the *Bekoma campechensis* Zone and subdivided it into three subzones based on materials from the northwest Atlantic. Hollis (1993, 1997, 2002) proposed a zonation for the lower Paleocene to middle Eocene in the mid-latitude of the South Pacific. Sanfilippo and Nigrini (1998a, b) proposed a tropical radiolarian zonation. Jackett *et al.* (2008) established an upper Paleocene to lower Eocene low-latitude radiolarian zonation based on re-sampled materials from DSDP Leg 43 Site 384 (Nishimura, 1992), ODP Leg 171B Hole 1051A (Sanfilippo and Blome, 2001), and DSDP Leg 10 Sites 86, 94, 95, and 96 (Foreman, 1973; Sanfilippo and Riedel, 1973). Norris *et al.* (2014) updated the low-latitude radiolarian zonal scheme of the lowermost Eocene through Upper Cretaceous (Sanfilippo and Nigrini, 1998b; Hollis, 2002) to the geological timescale 2012 (Gradstein *et al.*, 2012) based on correlation with calcareous microfossil datums. These publications on the Paleocene to lower Eocene radiolarian biostratigraphy (Figure 5) provide a sufficient standard for comparison and age assignment. In this study, the age assignment is based on low-latitude radiolarian zonation that was updated by Norris *et al.* (2014). Radiolarian assemblages in this study are comparable with the *Bekoma campechensis* Zone (RP6). The base of the RP6 is defined by the first appearance (FA) of *Bekoma campechensis* Foreman. The top of this zone is defined by the evolutionary transition from *B. campechensis* Foreman to *Bekoma bidartensis* Riedel and Sanfilippo (Nishimura, 1987, 1992; Sanfilippo and Nigrini, 1998b). The RP6 is divided into three subzones by the differences of the associated species. Our radiolarian assemblages are assigned

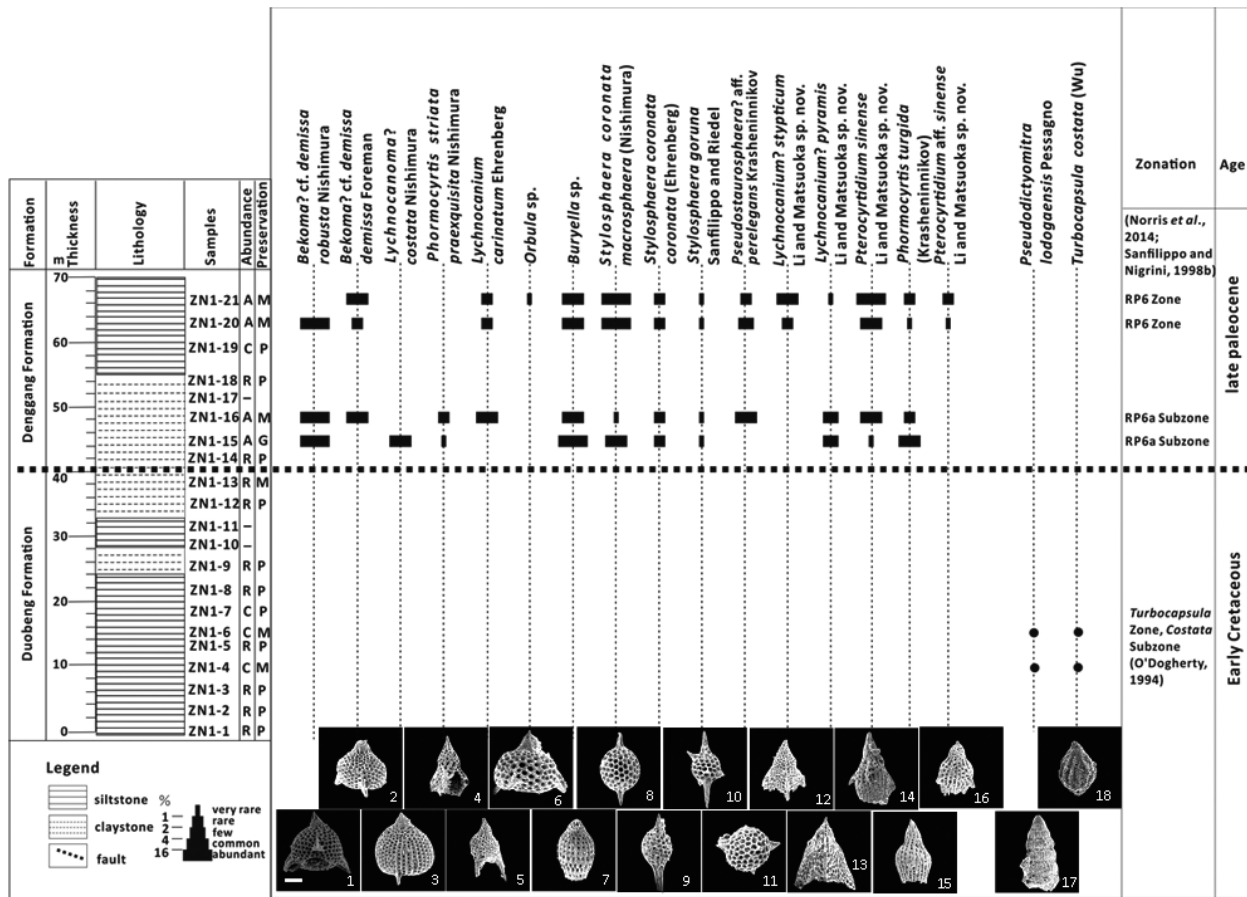


Figure 4. Columnar section with radiolarian range chart (scale bar is 50 μ m). Zonation of Early Cretaceous radiolarians is based on O'Dogherty (1994) and zonation of late Paleocene radiolarians is based on Sanfilippo and Nigrini (1998b).

to the zonal scheme according to the co-occurrence of some diagnostic species instead of zonal markers. The composite stratigraphic ranges of the diagnostic species referred to in this study are based on Foreman (1973), Nishimura (1992), and Sanfilippo and Nigrini (1998a, b).

Sample ZN1-15 yields *Lychnocanoma? costata* Nishimura, *Bekoma? cf. demissa robusta* Nishimura, *Phormocyrtis striata praexquisita* Nishimura, *Phormocyrtis turgida* (Krasheninnikov), *Lychnocanium? pyramis* Li and Matsuoka sp. nov., *Pterocyrtidium sinense* Li and Matsuoka sp. nov., *Buryella tetradica* Foreman s.s., *Buryella pentadica* Foreman, *Buryella* sp. A, *Stylosphaera coronata coronata* Ehrenberg, *Stylosphaera coronata macrosphaera* Nishimura, *Stylosphaera goruna* Sanfilippo and Riedel, *Amphisphaera minor* (Clark and Campbell), *Orbula* sp. A, *Stylotrachus* sp., *Cromyechinus* sp., and *Tripocalpis* sp. (Figures 4, 6–9). *Buryella tetradica* Foreman s.s., *B. pentadica* Foreman, *S. coronata coronata* Ehrenberg, and *S. goruna* Sanfilippo and Riedel are common species dur-

ing the late Paleocene to the early Eocene. *Phormocyrtis striata praexquisita* Nishimura and *L.? costata* Nishimura are species restricted to the *Bekoma campechensis* Zone, RP6a Subzone of Sanfilippo and Nigrini (1998b), indicating an age of 61.5–60.4 Ma (Norris et al., 2014) (Figure 10).

Sample ZN1-16 yields *Bekoma? cf. demissa robusta* Nishimura, *B.? cf. demissa demissa* Foreman, *Phormocyrtis striata praexquisita* Nishimura, *Lychnocanoma carinatum* Ehrenberg, *Phormocyrtis turgida* (Krasheninnikov), *Pterocyrtidium sinense* Li and Matsuoka sp. nov., *Lychnocanium? pyramis* Li and Matsuoka sp. nov., *Stylosphaera coronata coronata* Ehrenberg, *S. coronata macrosphaera* Nishimura, *Pseudostaurosphaera? aff. perelegans* Krasheninnikov, and *S. goruna* Sanfilippo and Riedel (Figures 4, 6–9). *Stylosphaera coronata coronata* Ehrenberg, *S. coronata macrosphaera* Nishimura, and *S. goruna* Sanfilippo and Riedel are common species during the late Paleocene to the early Eocene. The occurrence of *Phormocyrtis striata praexquisita* Nishimura indicates

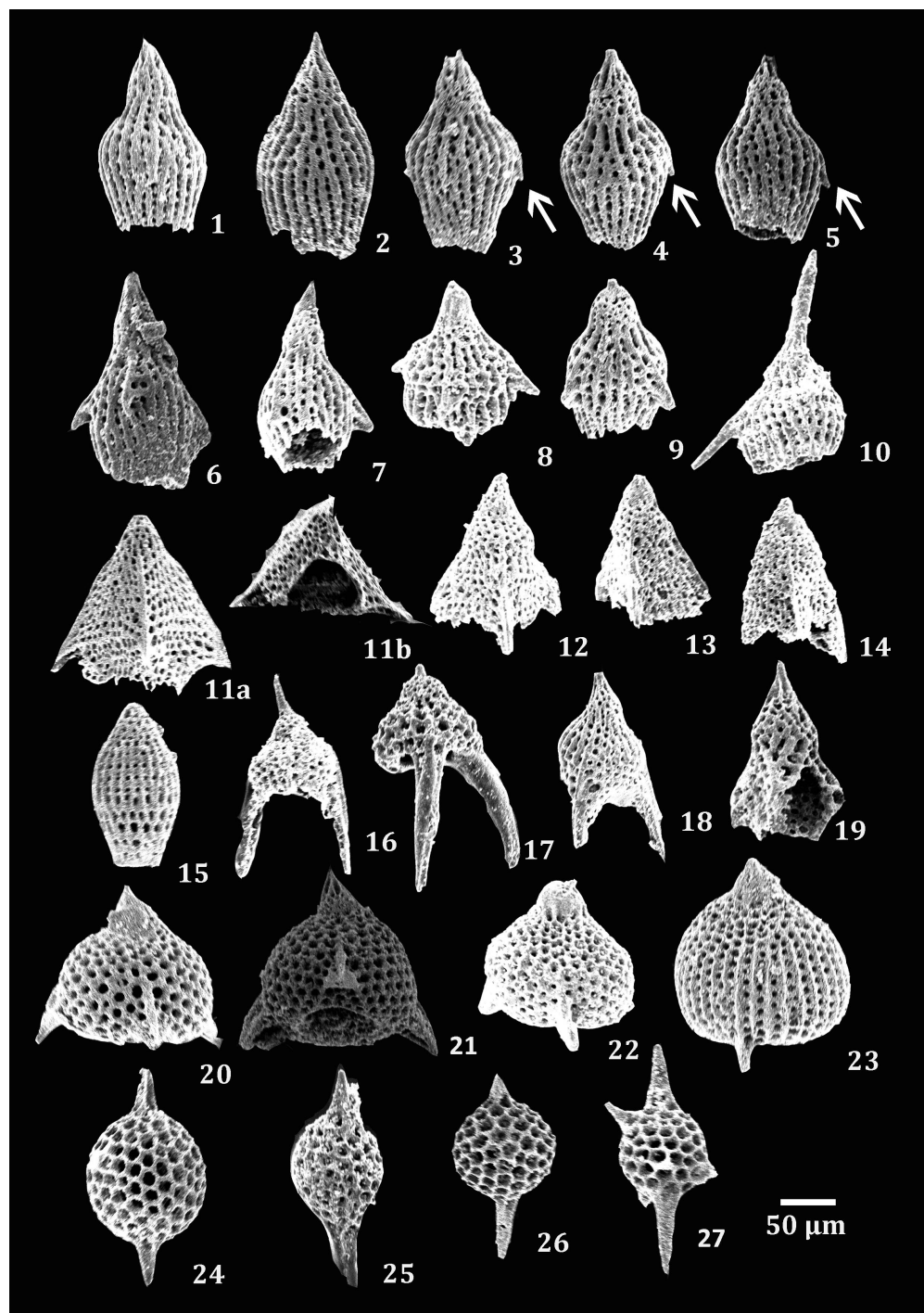


Figure 6. Scanning electron microscopic images of Paleocene radiolarians. **1, 2**, *Phormocyrtis turgida* (Krasheninnikov), ZN1-15; **3–5**, *Pterocyrtidium sinense* Li and Matsuoka sp. nov., transitional forms between *P. turgida* (Krasheninnikov) and *P. sinense* Li and Matsuoka sp. nov., ZN1-15; **6–8**, *Pterocyrtidium sinense* Li and Matsuoka sp. nov.; **6**, holotype, ZN1-16; **7**, paratype, ZN1-20; **8**, ZN1-21; **9, 10**, *Pterocyrtidium* aff. *sinense* Li and Matsuoka sp. nov.; **9**, ZN1-20; **10**, ZN1-21; **11**, *Lychnocanium? pyramis* Li and Matsuoka sp. nov., holotype; **11a**, lateral view, showing the constricted aperture on the fifth segment, ZN1-15; **11b**, basal view, showing the constricted aperture on the fifth segment, ZN1-15; **12–14**, *Lychnocanium? stypticum* Li and Matsuoka sp. nov., ZN1-21; **14**, holotype; **15**, *Buryella tetradica* Foreman var. A, ZN1-15; **16**, *Lychnocanoma* sp., ZN1-20; **17**, *Lychnocanoma anacolum* Foreman, ZN1-20; **18**, *Lychnocanium carinatum* Ehrenberg, ZN1-20; **19**, *Phormocyrtis striata praexquisita* Nishimura, ZN1-15; **20**, *Orbula* sp. A, ZN1-15; **21**, *Bekoma? cf. demissa robusta* Nishimura, ZN1-15; **22**, *Bekoma? cf. demissa demissa* Foreman, ZN1-20; **23**, *Lychnocanoma? costata* Nishimura, ZN1-15; **24**, *Stylosphaera coronata macrosphaera* Nishimura, ZN1-15; **25, 26**, *Stylosphaera coronata coronata* Ehrenberg; **25**, ZN1-15; **26**, ZN1-20; **27**, *Stylosphaera goruna* Sanfilippo and Riedel, ZN1-15. Arrows indicate small wings.

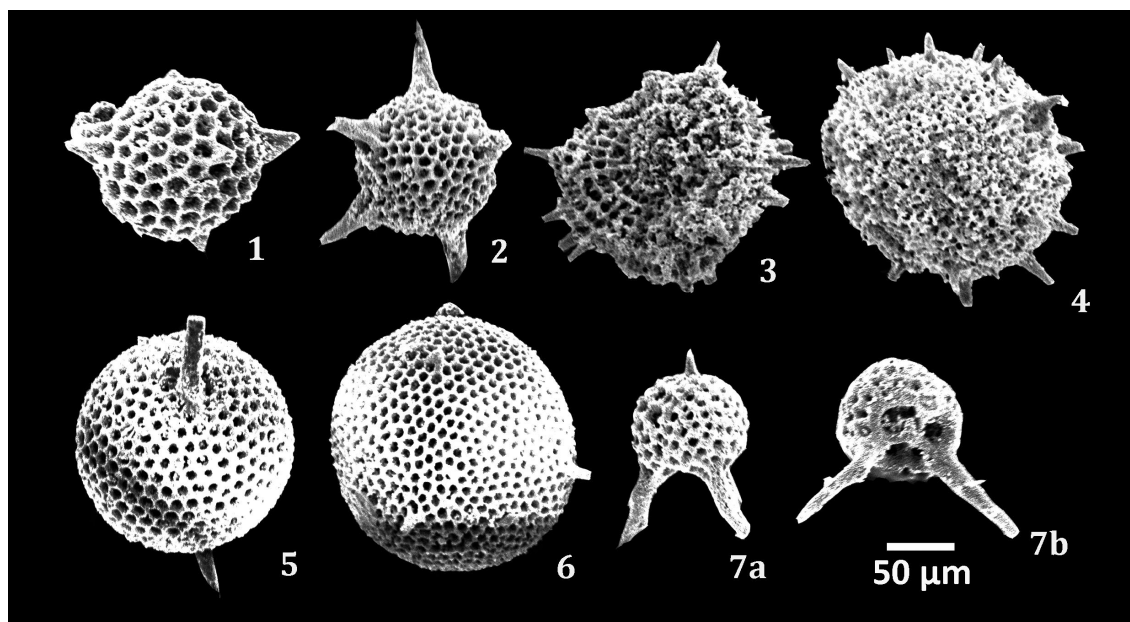


Figure 7. Scanning electron microscopic images of Paleocene radiolarians. 1, *Pseudostaurosphaera?* aff. *perelegans* Krasheninnikov, ZN1-20; 2, *Pseudostaurosphaera* sp., ZN1-20; 3, 4, *Stylotrochus* sp., ZN1-15; 5, *Amphisphaera minor* (Clark and Campbell), ZN1-15; 6, *Cromyechinus* sp., ZN1-15; 7, *Tripocalpis* sp., ZN1-15.

that the radiolarian assemblage is comparable with the *Bekoma campechensis* Zone, RP6a Subzone of Sanfilippo and Nigrini (1998b) with an age of 61.5–60.4 Ma (Norris *et al.*, 2014) (Figure 10).

Sample ZN1-20 yields *Bekoma?* cf. *demissa robusta* Nishimura, *B.?* cf. *demissa demissa* Foreman, *Lychnocanoma carinatum* Ehrenberg, *Lychnocanoma anacolum* Foreman, *Phormocyrtis turgida* (Krasheninnikov), *Lychnocanium?* *stypticum* Li and Matsuoka sp. nov., *Pterocyrtidium sinense* Li and Matsuoka sp. nov., *P.* aff. *sinense* Li and Matsuoka sp. nov., *Stylosphaera coronata coronata* Ehrenberg, *S. coronata macrosphaera* Nishimura, *S. goruna* Sanfilippo and Riedel, *Pseudostaurosphaera?* aff. *perelegans* Krasheninnikov, and *Stylotrochus* sp. (Figures 4, 6–9). The co-occurrence of *Lychnocanoma anacolum* Foreman, *Stylosphaera coronata coronata* Ehrenberg, and *S. coronata macrosphaera* Nishimura indicates that the radiolarian assemblage is restricted to the *Bekoma campechensis* Zone of Sanfilippo and Nigrini (1998b) with an age range of 61.5–58.23 Ma (Norris *et al.*, 2014) (Figure 10).

Sample ZN1-21 yields *Bekoma?* cf. *demissa demissa* Foreman, *Phormocyrtis turgida* (Krasheninnikov), *Lychnocanoma carinatum* Ehrenberg, *Lychnocanium?* *pyramis* Li and Matsuoka sp. nov., *Lychnocanium?* *stypticum* Li and Matsuoka sp. nov., *Pterocyrtidium sinense* Li and Matsuoka sp. nov., *P.* aff. *sinense* Li and Matsuoka sp. nov., *Pseudostaurosphaera?* aff. *perelegans* Krash-

eninnikov, *Stylosphaera coronata coronata* Ehrenberg, *S. coronata macrosphaera* Nishimura, and *S. goruna* Sanfilippo and Riedel (Figures 4, 6–9). The co-occurrence of *S. coronata coronata* Ehrenberg and *S. coronata macrosphaera* Nishimura indicates the radiolarian assemblage is restricted to the *Bekoma campechensis* Zone of Sanfilippo and Nigrini (1998b) with an age of 61.5–58.23 Ma (Norris *et al.*, 2014) (Figure 10).

Within the species stated above, the three new species (*Lychnocanium?* *pyramis* Li and Matsuoka sp. nov., *L.?* *stypticum* Li and Matsuoka sp. nov., and *Pterocyrtidium sinense* Li and Matsuoka sp. nov.) that occur in our samples (Figures 4, 6–8) have been sparsely reported in previous studies of other areas.

Discussion

Tectonic attributes and distribution

In the previous 1:250,000 geological map, the strata located to the south of the Yarlung-Tsangpo River near Zhongba County was mapped as Upper Cretaceous to middle Eocene sediments. As the map shows, upper Paleocene strata of the Denggang Formation are widely distributed in this area. According to our field investigations and radiolarian analyses, the strata are divided into the Weimei Formation (quartz sandstones), the Rilang Formation (volcaniclastic sandstones), the Duobeng Formation (siliceous mudstones interbedded with claystones),

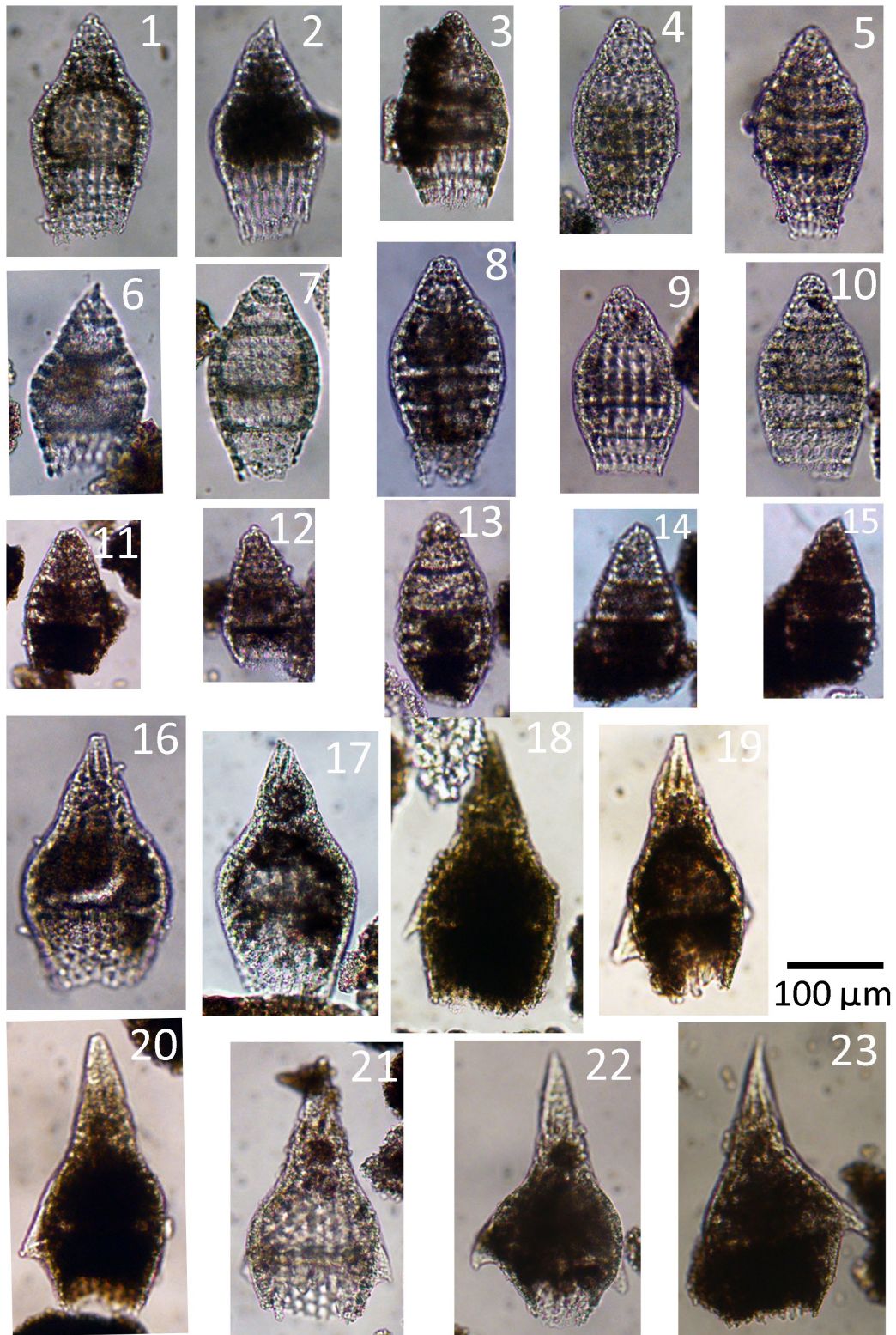


Figure 8. Light microscopic images of Paleocene radiolarians. **1, 2**, *Buryella pentadica* Foreman, ZN1-15; **3–5**, *Buryella* sp. A, ZN1-15; **6**, *Buryella tetradica* Foreman s.s., ZN1-15; **7–10**, *Buryella tetradica* Foreman var. A, ZN1-15; **11–15**, *Buryella* sp., 11–13, ZN1-20; 14, 15, ZN1-21; **16, 17**, *Phormocyrtis turgida* (Krasheninnikov), ZN1-15; **18–23**, *Pterocyrtidium sinense* Li and Matsuoka sp. nov.; 18, ZN1-16; 19–23, ZN1-20.

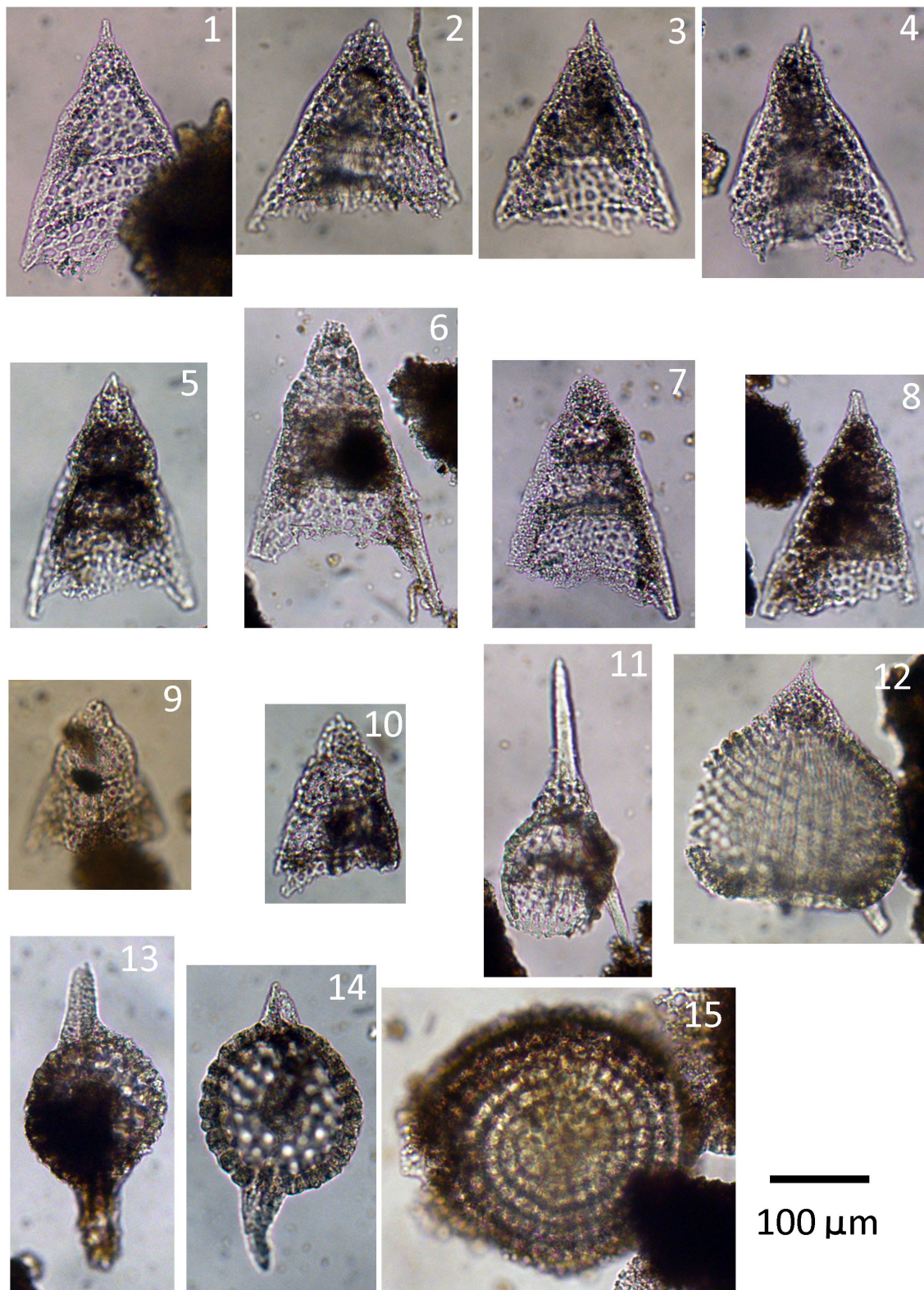


Figure 9. Light microscopic images of Paleocene radiolarians. 1–4, *Lychnocanium? pyramis* Li and Matsuoka sp. nov., ZN1-15; 4, paratype; 5–10, *Lychnocanium? stypticum* Li and Matsuoka sp. nov.; 5, ZN1-20; 6–10, ZN1-21; 7, paratype; 11, *Pterocyrtidium* aff. *sinense* Li and Matsuoka sp. nov., ZN1-21; 12, *Lychnocanoma? costata* Nishimura, ZN1-15; 13, *Stylosphaera coronata coronata* Ehrenberg, ZN1-20; 14, *Stylosphaera coronata macrosphaera* Nishimura, ZN1-20; 15, *Stylotrachus* sp., ZN1-20.

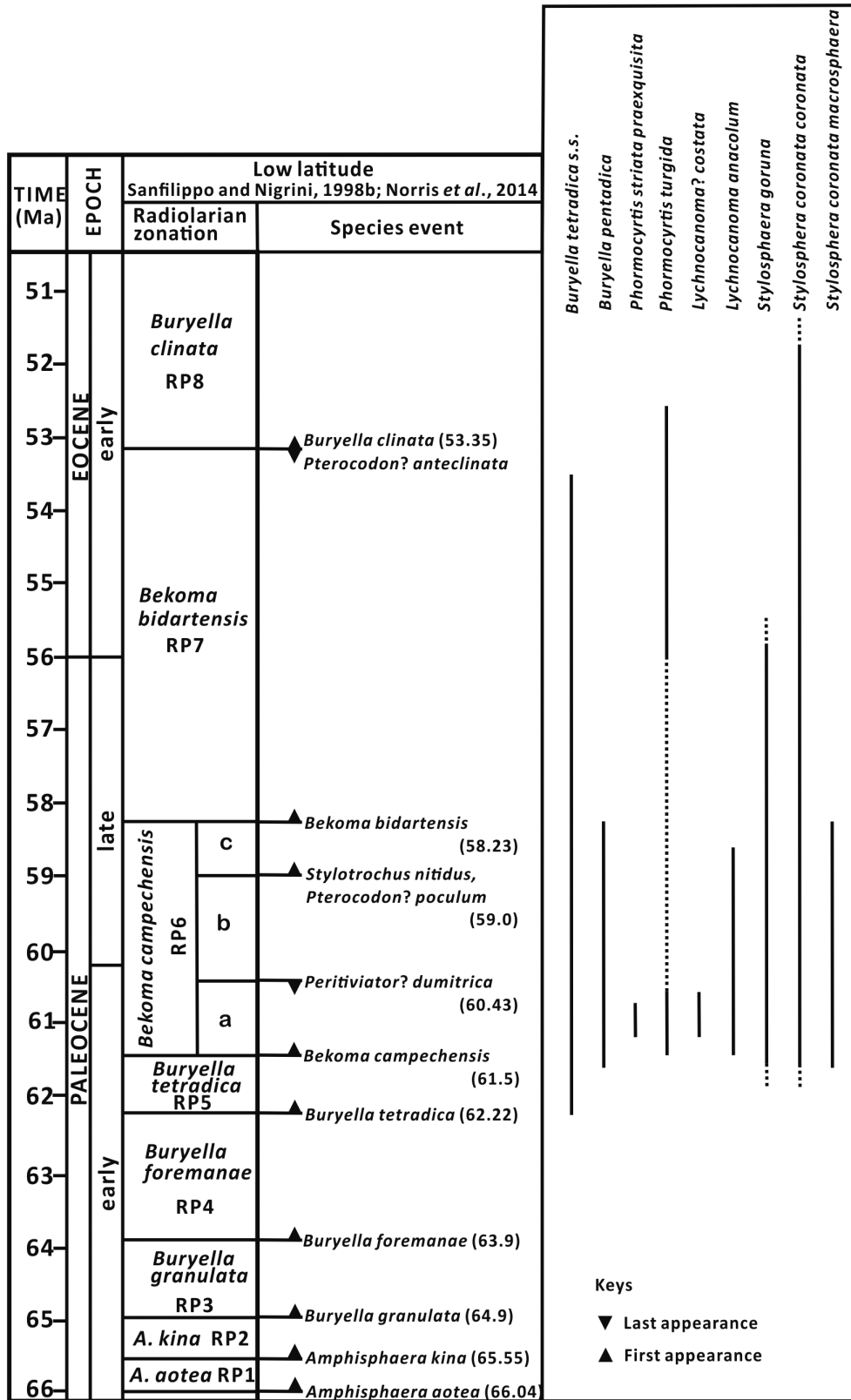


Figure 10. Stratigraphic ranges of diagnostic radiolarian species. Range of each species is based on Foreman (1973), Nishimura (1992), Sanfilippo and Nigrini (1998a, b), and Norris et al. (2014).

the Chuangde Formation (red limestones), and the Denggang Formation (siliceous siltstone and claystone). Geochronological data show that the youngest detrital zircons in the lowest volcanoclastic sandstones of the Rilang Formation have a U–Pb age of $(134 \pm 4 \text{ Ma})$ (Du *et al.*, 2015). Radiolarians of Late Jurassic and Early Cretaceous age can be found in the upper part of the Rilang Formation and the Duobeng Formation (Li *et al.*, 2017). The majority of the strata are sediments belonging to these four Mesozoic formations instead of Upper Cretaceous to middle Eocene flysches. The upper Paleocene radiolarian-bearing siliceous mudstones, as the map shows, are not widely distributed, but only preserved in the southern part of these four formations. The upper Paleocene siliceous mudstone (20 m thick) is in fault contact with the Lower Cretaceous siliceous mudstone (Figures 3, 4).

Depositional environment of upper Paleocene radiolarian-bearing strata

Radiolarians are planktonic protozoa that are widely distributed in the oceans, throughout the water column from the near surface to the bottom.

Upper Paleocene radiolarian-bearing strata are the latest marine sediments recorded near Zhongba County. Mesozoic to Paleogene deep-marine sediments (Liu and Einsele, 1994) change southward into shallow-water calcareous and terrigenous rocks (Willems *et al.*, 1996; Ding, 2003) on the Indian passive margin. The upper Paleocene radiolarian-bearing strata near Zhongba County stand for deep-marine sediments.

Liu and Aitchison (2002) remarked that the radiolarian faunas from the Yamdrok mélange correspond to the *Bekoma campechensis* Zone of Nishimura (1992). Ding (2003) assigned radiolarian assemblages from the Zheba section as the *Buryella tetradica* Zone (RP5) and the *Bekoma campechensis* Zone (RP6), inferring a time interval of 61–55 Ma. Liang *et al.* (2012) assigned the radiolarian assemblage from the Jiazhu section to the *Buryella pentadica* Zone (RP6) of Hollis (2002), indicating an equivalent age of 59–56.5 Ma. Radiolarian assemblages from the three locations are comparable with the *Bekoma campechensis* Zone (RP6) of Sanfilippo and Nigrini (1998b), indicating an age range of 61.5–58.23 Ma based on the updated zonal scheme of Norris *et al.* (2014) (Figures 5, 10).

The Jiazhu section is 4 km west of the ZN1 section, which is 200 km west of the Zheba section (Figure 1). The ZN1 section and Jiazhu section (Liang *et al.*, 2012) consist of siliceous mudstones and cherts, which lack any calcareous and coarse-grained terrestrial materials. These strata stand for deep-marine sediments deposited below the calcium carbonate compensation depth (CCD). The Zheba section consists of gray-white cherts, porcellanites,

siliceous shales, siliceous limestones, and conglomerates. The coexistence of limestones and radiolarian-bearing porcellanites is evidence that sediments near Zheba were accumulated in a relatively shallower depth near the CCD. The conglomerate might be related to the initial collision between the Indian and the Eurasian continents. The lack of coarse-grained terrestrial sediments near Zhongba provides additional information that the marine basin here was more distal to the continents than that near Zheba.

Further to the east near Gyangze, olistostromes and chaotic deposits, which contain clasts from the passive continental margin, the oceanic crust, and the active continental margin, were accumulated during the late Paleocene (Liu and Einsele, 1996; Liu and Aitchison, 2002). The olistostromes and chaotic deposits stand for the trench basin sediments developed during the collision.

The lateral variations in the lithology indicate that the strata near Zhongba, Zheba, and Gyangze were deposited in marginal areas with different water depths and distances to the continents during the late Paleocene.

Conclusions

Radiolarian assemblages from a deep-marine succession of siliceous siltstone and claystone can be correlated to the *Bekoma campechensis* Zone (RP6) of Sanfilippo and Nigrini (1998b) with an age range of 61.5–58.23 Ma. This succession represents a record of deep-marine sediments on the Indian passive margin near Zhongba County. The distribution of the late Paleocene radiolarian-bearing strata is limited to the southern part of the deep-marine sediments. The radiolarian assemblages of the Yamdrok mélange (Liu and Aitchison, 2002), the Zheba section (Ding, 2003), and the Jiazhu section (Liang *et al.*, 2012) indicate the same age as those of the ZN1 section. The sediments were deposited below the CCD near Zhongba. Compared with coeval sediments of the NTH, the deep-marine realm near Zhongba was deeper and more distal than that near Saga and Gyangze.

Systematic paleontology

Full description is given for new species and species for which taxonomic clarification is required. For other species, reference to the author, the first illustration, and the currently adopted species concept are given. Genera and species are arranged in alphabetical order within orders Spumellaria and Nassellaria, respectively.

Superorder Polycystina Ehrenberg, 1838, emend. Riedel, 1967

Order Spumellaria Ehrenberg, 1875

Genus *Amphisphaera* Haeckel, 1881, emend.

Petrushevskaya, 1975

Type species.—*Amphisphaera neptunus* Haeckel, 1887.

Amphisphaera minor (Clark and Campbell, 1942)

Figure 7.5

Stylosphaera minor Clark and Campbell, 1942, p. 27, pl. 5, figs. 1, 2, 12.

Amphisphaera minor (Clark and Campbell). Sanfilippo and Riedel, 1973, p. 486, pl. 1, figs. 1–5, pl. 22, fig. 4.

Remarks.—Our specimen is identified as *A. minor* (Clark and Campbell) by having a shell with two opposite similar basally three-bladed, narrow, needlelike polar spines. The polar spines of the specimen examined here are broken. The cortical shell of our specimen is larger than those reported by Clark and Campbell (1942), which is 100 µm in diameter.

Occurrence.—Upper Paleocene in North Atlantic (Nishimura, 1987; Jackett *et al.*, 2008; Liu *et al.*, 2011), Gulf of Mexico (Sanfilippo and Riedel, 1973), New Zealand (Hollis, 2006), South Africa (Jannou, 2007), California (Clark and Campbell, 1942), and Tibet.

Genus ***Pseudostaurosphaera*** Krasheninnikov, 1960

Type species.—*Pseudostaurosphaera perelegans* Krasheninnikov, 1960.

Pseudostaurosphaera?* aff. *perelegans Krasheninnikov, 1960

Figure 7.1

Pseudostaurosphaera perelegans Krasheninnikov, 1960, p. 276, pl. 1, fig. 6.

Pseudostaurosphaera? aff. *perelegans* Krasheninnikov. Nishimura, 1992, pl. 1, fig. 5.

Remarks.—The specimens in this study should be conspecific with *Pseudostaurosphaera?* aff. *perelegans* Krasheninnikov reported by Nishimura (1992, pl. 1, fig. 5). Specimens of this species in Tibet reported by Liang *et al.* (2012, fig. 3a, 3b) were assigned to *Hexacantium? palaeocenicum* Sanfilippo and Riedel, 1973. This species differs from *P. perelegans* Krasheninnikov and *H.? palaeocenicum* Sanfilippo and Riedel by having more numerous and smaller pores.

Occurrence.—Upper Paleocene in Northeast Atlantic (Nishimura, 1992) and Tibet (Liang *et al.*, 2012).

Genus ***Stylosphaera*** Ehrenberg, 1847

Type species.—*Stylosphaera hispida* Ehrenberg, 1854

(designated by Campbell, 1954).

Stylosphaera coronata coronata Ehrenberg, 1873

Figures 6.25, 6.26, 9.13

Stylosphaera coronata Ehrenberg, 1873, p. 258; Ehrenberg, 1875, pl. 25, fig. 4.

Stylosphaera coronata coronata Ehrenberg. Sanfilippo and Riedel, 1973, p. 520, pl. 1, figs. 13–17, pl. 25, fig. 4.

Remarks.—Our specimens are identified as this subspecies by having a spherical or elliptical outer shell with two three-bladed polar spines.

Occurrence.—Upper Paleocene in North Atlantic (Nishimura, 1992; Jackett *et al.*, 2008; Liu *et al.*, 2011), Japan (Oyaizu *et al.*, 2002), New Zealand (Hollis, 2006), and Tibet (Liu and Aitchison, 2002; Liang *et al.*, 2012).

Stylosphaera coronata macrosphaera Nishimura, 1992

Figures 6.24, 9.14

Stylosphaera coronata macrosphaera Nishimura, 1992, p. 325, pl. 1, figs. 3, 4, pl. 11, fig. 1.

Remarks.—Specimens examined here identified as *S. coronata macrosphaera* Nishimura differ from *S. coronata coronata* Ehrenberg by having a larger outer shell and shorter polar spines.

Occurrence.—Upper Paleocene in North Atlantic (Nishimura, 1992; Jackett *et al.*, 2008; Liu *et al.*, 2011), and Tibet (Liu and Aitchison, 2002; Liang *et al.*, 2012).

Stylosphaera goruna Sanfilippo and Riedel, 1973

Figure 6.27

Stylosphaera goruna Sanfilippo and Riedel, 1973, p. 521, pl. 1, figs. 20–22, pl. 25, figs. 9, 10.

Remarks.—Our specimens are identified as *S. goruna* Sanfilippo and Riedel by having a cortical shell with two or more spines at or near each pole. This species includes variable forms with different size and thickness of the outer shell and different length of radial spines.

Occurrence.—Upper Paleocene and lower Eocene in North Atlantic (Nishimura, 1992; Jackett *et al.*, 2008; Liu *et al.*, 2011), Japan (Nanayama, 1992; Oyaizu *et al.*, 2002), Canary Islands (Bustillo *et al.*, 1994), New Zealand (Hollis and Hanson, 1991; Hollis, 1993; Strong *et al.*, 1995), South Africa (Jannou, 2007), and Tibet (Liu and Aitchison, 2002; Liang *et al.*, 2012).

Order Nasselaria Ehrenberg, 1875

Genus ***Bekoma*** Riedel and Sanfilippo, 1971

Type species.—*Bekoma bidartensis* Riedel and Sanfilippo, 1971.

***Bekoma?* cf. *demissa demissa* Foreman, 1973**

Figure 6.22

Bekoma? demissa Foreman, 1973, p. 432, pl. 3, fig. 22, pl. 10, fig. 5.
Bekoma? demissa Foreman. Nishimura, 1992, p. 333, pl. 6, fig. 1.

Remarks.—Specimens examined in this study are doubtfully identified as *Bekoma? cf. demissa demissa* by lacking typical long conical feet that extend out from the lower part of the thorax. Specimens examined in this study is similar to *B.? cf. demissa demissa* in having a hemispherical cephalis and a campanulate, thick-walled thorax with small pores regularly arranged.

Occurrence.—Upper Paleocene in Tibet.

***Bekoma?* cf. *demissa robusta* Nishimura, 1992**

Figure 6.21

Bekoma? demissa robusta Nishimura, 1992, p. 333, pl. 6, figs. 2, 3.

Remarks.—Our specimens are doubtfully identified as *Bekoma? cf. demissa robusta* by lacking typical long conical feet that extend out from the lower part of the thorax. This specimen is different form *B.? cf. demissa demissa* (Figure 6.21) by having a rather campulate, not roundish thorax.

Occurrence.—Upper Paleocene in Tibet (Liang *et al.*, 2012).

Genus ***Buryella*** Foreman, 1973

Type species.—*Buryella tetradica* Foreman, 1973.

***Buryella pentadica* Foreman, 1973**

Figures 8.1, 8.2

Buryella pentadica Foreman, 1973, p. 433, pl. 8, fig. 8, pl. 9, figs. 15, 16.

Remarks.—This species differs from *Buryella tetradica* Foreman *s.s.* by the number and size of segments. *Buryella pentadica* has an inverted truncate-conical fifth segment, while *B. tetradica* has four segments. They both have a small cephalis. The thorax of *B. pentadica* is smaller than that of *B. tetradica* Foreman *s.s.* The abdomen of *B. pentadica* is truncated-conical, while the abdomen of *B. tetradica* Foreman *s.s.* is inflated cylindrical. The fourth segment of *B. pentadica* is similar to the abdomen of *B. tetradica* Foreman *s.s.* The fourth segment of *B. tetradica* is inverted truncate-conical. The thorax and abdomen of this species is smaller compared with *B.*

tetradica Foreman *s.s.*, *B. tetradica* Foreman var. A, and *B. sp. A*. The fourth segment is more inflated and bigger than that of *B. tetradica* Foreman *s.s.*, *B. tetradica* Foreman var. A, and *B. sp. A*.

Occurrence.—Upper Paleocene in Gulf of Mexico (Foreman, 1973), North Atlantic (Nishimura, 1992; Liu *et al.*, 2011), South Pacific (O'Connor, 2001), Cuba (Sanfilippo *et al.*, 1999), Canary Islands (Bustillo *et al.*, 1994), and Tibet (Ding, 2003; Liang *et al.*, 2012).

Buryella tetradica* Foreman, 1973 *sensu stricto

Figure 8.6

Buryella tetradica Foreman, 1973, p. 433, pl. 8, figs. 4, 5, pl. 9, figs. 13, 14.

Buryella tetradica Foreman *s.s.* Sanfilippo and Blome, 2001, p. 210.

Remarks.—*Buryella tetradica* Foreman *s.s.* and *B. tetradica* Foreman var. A are two subspecies of *B. tetradica*. These two subspecies have similar cephalis, thorax, and abdomen.

Occurrence.—Upper Paleocene to lower Eocene in Gulf of Mexico (Foreman, 1973; Jackett *et al.*, 2008), South Pacific (O'Connor, 2001), North Atlantic (Nishimura, 1992; Sanfilippo and Blome, 2001; Liu *et al.*, 2011), Cuba (Sanfilippo *et al.*, 1999), northern Cyprus (Sanfilippo *et al.*, 2003), Canary Islands (Bustillo *et al.*, 1994), New Zealand (Hollis, 2006; Strong *et al.*, 1995), and Tibet (Liang *et al.*, 2012).

***Buryella tetradica* Foreman var. A**

Figures 6.15, 8.7–8.10

Buryella tetradica Foreman var. A. Sanfilippo and Blome, 2001, p. 210, figs. 8d, 8e.

Remarks.—*Buryella tetradica* Foreman var. A differs from *B. tetradica* Foreman *s.s.* by having a fourth segment which is transversely segmented. The differences of this species from *B. pentadica* Foreman and *B. sp. A* are described under those species.

Occurrence.—Upper Paleocene in North Atlantic (Sanfilippo and Blome, 2001) and Tibet.

***Buryella* sp. A**

Figures 8.3–8.5, 8.11–8.15

Buryella sp. A. Jackett *et al.*, 2008, p. 47, pl. 1, figs. 21–23.

Remarks.—This species differs from *Buryella tetradica* Foreman *s.s.* by having five segments. This species differs from *B. tetradica* Foreman var. A and *B. pentadica* Foreman by the third and fourth segments displaying similar proportions. The third segment of *B. tetradica*

Foreman var. A is more inflated and larger than the fourth segment. The third segment of *B. pentadica* Foreman is smaller than the fourth segment.

Occurrence.—Upper Paleocene in Northwest Atlantic (Jackett *et al.*, 2008) and Tibet.

Genus *Lychnocanium* Ehrenberg, 1847

Type species.—*Lychnocanium falciferum* Ehrenberg, 1854.

Lychnocanium carinatum Ehrenberg, 1875

Figure 6.18

Lychnocanium carinatum Ehrenberg, 1876, p. 78, pl. 8, fig. 5.

Remarks.—For the specimen of Ehrenberg (1875), there are no pores in the upper part of the thorax. Our specimen has pores and costae in the whole thorax.

Occurrence.—Upper Paleocene to lower Eocene in Northeast Atlantic (Liu *et al.*, 2011), Gulf of Mexico (Jackett *et al.*, 2008), and Tibet (Liang *et al.*, 2012).

Lychnocanium? pyramis Li and Matsuoka sp. nov.

Figures 6.11, 9.1–9.4

Lithochytris sp. Oyaizu *et al.*, 2002, fig. 6.11.

Diagnosis.—Five-segmented Nassellaria characterized by having a trigonal pyramidal shell with an aperture. Pores are circular to subcircular, variable in size, and closely spaced on the post-cephalic segments. Three solid ribs extend externally from the lower part of the thorax.

Description.—Trigonal-pyramidal shell with five segments. Cephalis small, conical, with a short apical horn. Pores small, circular to subcircular, irregularly distributed. Collar stricture not expressed externally. Thorax truncated pyramidal. Lumbar stricture slightly distinct in contour. Abdomen and the fourth segment truncated-pyramidal. The fifth segment inverted truncated-pyramidal with a constricted triangular aperture on more complete specimens (Figure 6.11b). The fifth segment very delicate, generally only seen as small remnants (Figures 9.2, 9.3). All the post-cephalic segments with circular to subcircular, variable in size, and closely spaced pores. All the segments except the fifth one increase their size gradually and constitute a large trigonal pyramid. Three solid ribs distally diverging and externally visible from the lower part of the thorax along the edges of the abdomen and the fourth segment. As the fifth segment is inverted truncated-pyramidal and constricted distally, the three ribs extend below the fourth segment as three short feet.

Measurements (in μm , based on 6 specimens).—Total

height, 131–163 (mean, 147; holotype, 157; paratype, 136); Height of cephalis, 18–25 (mean, 22; paratype, 18); Height of thorax, 15–21 (mean, 19; paratype, 20); Height of abdomen, 27–43 (mean, 34; paratype, 27); Height of the fourth segment, 28–36 (mean, 33; paratype, 35); Maximum width, 119–160 (mean, 131; holotype, 160; paratype, 133); Angle between two ribs in lateral view, 41° – 56° (mean, 48° ; holotype, 56° ; paratype, 48°).

Remarks.—This species is questionably assigned to the genus *Lychnocanium*, because of its special trigonal-pyramidal morphology, more segments, and smaller thorax. This species is distinguished from species of the genus *Lithochytris* by having an open aperture. This species is distinguished from *Dictyocephalus middouri* Nishimura, 1992 by having a trigonal-pyramidal shell, constricted fifth segment, and closely spaced pores on the post-cephalic segments. This species has a close phyletic relationship with *Lychnocanium? stypticum* Li and Matsuoka sp. nov. Their relationship is described under the latter species.

Etymology.—This species name is derived from Greek *pyramis*, meaning the pyramids of Egypt.

Type specimens.—Holotype NU MR 0120 (Figure 6.11); paratype NU MR 0121 (Figure 9.4).

Occurrence.—Upper Paleocene in Japan (Oyaizu *et al.*, 2002) and Tibet.

Lychnocanium? stypticum Li and Matsuoka sp. nov.

Figures 6.12–6.14, 9.5–9.10

Diagnosis.—Five-segmented Nassellaria characterized by possessing a trigonal pyramidal shell with an aperture. The lumbar stricture is distinct in contour. Pores are circular to subcircular, variable in size, and closely spaced on the post-cephalic segments. Three solid ribs are externally visible from the lower part of the thorax.

Description.—Trigonal-pyramidal shell with five segments. Cephalis small conical, with a short apical horn, generally smooth surfaced. Pores, if present, small in number, circular to subcircular, irregularly distributed. Collar stricture slightly distinct in contour. Thorax inflated truncated-conical. Lumbar stricture marked by a distinct change in contour. Abdomen and the fourth segment truncated-pyramidal. The fifth segment very delicate, generally only seen as small remnants (Figures 9.5, 9.7). All the post-cephalic segments with circular to subcircular, variable in size, and closely spaced pores. All the segments except the fifth one increase their width gradually and constitute a large trigonal pyramid. Three solid ribs externally visible from the lower part of the thorax to the distal postabdomen. Shell terminated in a ragged margin.

Measurements (in μm , based on 24 specimens).—Total height, 115–173 (mean, 143; holotype, 166; paratype,

148); Height of cephalis, 17–25 (mean, 22; paratype, 22); Height of thorax, 29–42 (mean, 34; paratype, 29); Height of abdomen, 27–45 (mean, 36; paratype, 37); Height of the fourth segment, 25–40 (mean, 34; paratype, 38, based on 8 specimens); Maximum width, 86–137 (mean, 109; holotype, 122; paratype, 125); Angle between two ribs in lateral view, 23°–42° (mean, 34°; holotype, 42°; paratype, 38°).

Remarks.—The wall of the fourth and fifth segments is fragile and not preserved in some specimens (Figures 9.9, 9.10). This species is distinguished from *Lychnocanium? pyramis* Li and Matsuoka sp. nov. by having a larger thorax that is obviously inflated, well expressed lumbar stricture in contour, and smaller angle between two ribs in lateral view. This species differs from *Lychnocanium auxilla* Foreman in having five segments, a robust abdomen that is generally preserved, and thoracic ribs which are slightly visible. This species differs from *Dictyocephalus middouri* Nishimura in having a cross section which is triangular instead of circular and having pores which are smaller and closer distributed. This species may have evolved from *L.? pyramis* Li and Matsuoka sp. nov. by developing a larger and more inflated thorax and constricting the angles between adjacent ribs.

Etymology.—This species name is derived from Latin *stypticus*, meaning astringent.

Type specimens.—Holotype NU MR 0122 (Figure 6.12); paratype NU MR 0123 (Figure 9.7).

Occurrence.—Upper Paleocene in Tibet.

Genus *Lychnocanoma* Haeckel, 1887, emend. Foreman, 1973

Type species.—*Lychnocanium clavigerum* Haeckel, 1887 (designated by Campbell, 1954)

***Lychnocanoma anacolum* Foreman, 1973**

Figure 6.17

Lychnocanoma anacolum Foreman, 1973, p. 437, pl. 1, figs. 19, pl. 11, fig. 7.

Remarks.—Our specimens are identified as *L. anacolum* Foreman by having a thorax with large irregular pores, three-bladed feet with convexity outwards, and a horn.

Occurrence.—Upper Paleocene in Gulf of Mexico (Foreman, 1973) and Tibet.

***Lychnocanoma? costata* Nishimura, 1992**

Figures 6.23, 9.12

Lychnocanoma? costata Nishimura, 1992, p. 342, pl. 6, figs. 4–6.

Remarks.—Specimens examined in this study are identified as *L.? costata* Nishimura by having well developed costae and pores regularly arranged in longitudinal rows on the wide thorax.

Occurrence.—Upper Paleocene in Northwest Atlantic (Nishimura, 1987, 1992) and Tibet (Liu and Aitchison, 2002; Ding, 2003).

Genus ***Phormocyrtis* Haeckel, 1887**

Type species.—*Phormocyrtis longicornis* Haeckel, 1887 (designated by Campbell, 1954).

***Phormocyrtis striata praexquisita* Nishimura, 1992**

Figure 6.19

Phormocyrtis striata praexquisita Nishimura, 1992, p. 346, pl. 9, figs. 1–3.

Remarks.—Nishimura (1992) defined forms having well developed abdomen and convexly curved keels as this subspecies. This subspecies is located in a lower horizon than *Phormocyrtis striata exquisita* (Kozlova, 1966) (Foreman, 1973).

Occurrence.—Upper Paleocene in Northwest Atlantic (Nishimura, 1987, 1992) and Tibet.

***Phormocyrtis turgida* (Krasheninnikov, 1960)**

Figures 6.1, 6.2, 8.16, 8.17

Lithocampe turgida Krasheninnikov, 1960, p. 301, pl. 3, fig. 17.

Phormocyrtis turgida (Krasheninnikov). Foreman, 1973, p. 438, pl. 7, fig. 10, pl. 12, fig. 6; Nishimura, 1987, p. 727, pl. 2, fig. 12; Sanfilippo and Nigrini, 1998a, p. 273, pl. 13.2, fig. 3; Kozlova, 1999, ? pl. 15, fig. 7, pl. 20, figs. 13; Sanfilippo *et al.*, 1999, pl. 2, fig. 6; Nishimura, 2001, pl. 6, figs. 5, 25; Liu and Aitchison, 2002, p. 150, pl. 1, fig. 23; Sanfilippo *et al.*, 2003, p. 56, pl. 2, fig. 15; Hollis, 2006, pl.2, figs. 13, 14; Jackett *et al.*, 2008, p. 57, pl. 2, fig. 15.

Phormocyrtis cf. *turgida* (Krasheninnikov). Kozlova, 1999, ? p. 149, pl. 18, fig. 21; pl. 46, figs. 7, 8.

Phormocyrtis striata striata (Kozlova, 1999). Cluzel *et al.*, 2001, pl. 2, fig. D.

Phormocyrtis aff. *turgida* (Krasheninnikov). Nishimura, 2001, pl. 13, fig. 8.

Podocyrtis turgida Krasheninnikov. Ding, 2003, fig. 4.18.

Description.—Four-segmented, fusiform shell narrows in the aperture. No strictures expressed externally. Cephalis small, spherical, with a small and slightly bladed to conical apical horn. Pores circular to subcircular, various in size, and irregularly distributed. Collar stricture slightly distinct externally as change in contour. Thorax truncated conical. Lumbar stricture externally invisible. Abdomen large and inflated truncated-conical. The fourth segment inverted truncated-conical. Pores on the post-

cephalic segments, circular to subcircular, various in size, and with thick ribs between adjacent longitudinal rows of pores. Eleven to thirteen ribs in lateral view. Some ribs separate into two branches on the abdomen.

Remarks.—This species is assigned to the genus *Phormocyrtis* because it bears an apical horn and ribs from the thorax to the distal part. Specimens of this species from Tibet are characterized by having a larger cephalis, shorter thorax, and a more inflated overall shape than specimens reported in Foreman (1973, pl. 7, fig. 10; pl. 12, fig. 6) and Jackett *et al.* (2008, pl. 2, fig. 15), which are restricted to the early Eocene. Specimens of this species from Tibet are the same as the specimens reported by Nishimura (2001, pl. 6, figs. 5, 25; pl. 13, fig. 8), which are also of late Paleocene age. Our specimens differ from *Podocyrtis papalis* Ehrenberg, 1847 (Nishimura, 1992, pl. 10, fig. 1-2, pl. 13, fig. 18; Sanfilippo and Blome, 2001, fig. 10f) in having a less inflated overall shape and longer fourth segment. This species appears to be an early form of *P. papalis* Ehrenberg. This species has a close phyletic relationship with *Pterocyrtidium sinense* Li and Matsuoka sp. nov. Their relationship is described under that species.

Occurrence.—Upper Paleocene to lower Eocene in Cyprus (Sanfilippo *et al.*, 2003), Gulf of Mexico (Foreman, 1973; Jackett *et al.*, 2008), Atlantic (Nishimura, 1987), Southwest Pacific (Cluzel *et al.*, 2001), Caucasus (Krasheninnikov, 1960), Russia (Kozlova, 1999), Cuba (Sanfilippo *et al.*, 1999), New Zealand (Hollis, 2006), and Tibet (Liu and Aitchison, 2002; Ding, 2003).

Genus *Pterocyrtidium* Bütschli, 1882, *sensu*
Petrushevskaya and Kozlova, 1972

Type species.—*Pterocanium barbadensis* Ehrenberg, 1873 (designated by Petrushevskaya and Kozlova, 1972)

Pterocyrtidium sinense Li and Matsuoka sp. nov.

Figures 6.3–6.8, 8.18–8.23

Calocyrtella tibeta Ding, 2003, figs. 4.4, 4.5; Liang *et al.*, 2012, figs. 4.a, 4.b.

Diagnosis.—A *Pterocyrtidium* species characterized by possessing a four-segmented, fusiform shell. Three latticed, triangular wings extend outwards and downwards from the lower part of the abdomen. Thick ribs are distributed between adjacent longitudinal rows of pores on the post-cephalic segments.

Description.—Four-segmented, fusiform shell narrow distally. Cephalis small, spherical, sparsely perforate with circular to subcircular, various in size, and irregularly distributed pores. Apical horn small and slightly bladed to

conical. Collar stricture externally distinct as change in contour. Thorax small truncated conical. Lumbar stricture usually externally invisible. Abdomen large and inflated truncated-conical. Three latticed, triangular wings spaced equally around the lower part of the abdomen, extending outwards and downwards. The fourth segment inverted truncated-conical and terminated in a ragged margin. Pores on the post-cephalic segments, circular to subcircular, various in size, and with thick ribs between adjacent longitudinal rows of pores. Eleven to thirteen ribs in lateral view. Some ribs separating into two branches on the abdomen.

Measurements (in μm , based on 35 specimens).—Total height, 147–227 (mean, 188; holotype, 193; paratype, 166); maximum width, 77–103 (mean, 91; holotype, 92; paratype, 88).

Remarks.—*Pterocyrtidium sinense* (Figure 6.8) differs from *Pterocyrtidium genriettae* Nishimura, 1992 by having obvious costae on the thorax and a shorter abdomen. This species is similar to *Phormocyrtis turgida* (Krasheninnikov) in overall shape, pore arrangement, and ribs. This species differs from *P. turgida* (Krasheninnikov) by having three latticed, triangular wings in the thorax. *Pterocyrtidium sinense* Li and Matsuoka sp. nov. can be regarded as a descendant of *P. turgida* (Krasheninnikov) tentatively and seems to be derived from the latter species by acquiring three latticed, triangular wings on the abdomen. Transitional forms between these two species have smaller wings than *P. sinense* Li and Matsuoka (Figures 6.3–6.5). These *P. sinense* Li and Matsuoka with smaller wings are found only in sample ZN1-15. *Phormocyrtis turgida* (Krasheninnikov) is dominant in this sample. In samples ZN1-16, ZN1-20, and ZN1-20, *P. sinense* Li and Matsuoka becomes dominant, while rare specimens of *P. turgida* (Krasheninnikov) are found.

Type specimens.—Holotype NU MR 0124 (Figure 6.6); paratype NU MR 0125 (Figure 6.7).

Occurrence.—Upper Paleocene in Tibet (Ding, 2003; Liang *et al.*, 2012).

Pterocyrtidium aff. *sinense* Li and Matsuoka sp. nov.

Figures 6.9, 6.10, 9.11

Pterocyrtidium cf. *genriettae* Nishimura. Liang *et al.*, 2012, figs. 11v, 11w.

Remarks.—This species is different from *Pterocyrtidium sinense* Li and Matsuoka sp. nov. by having a larger and more inflated cephalis. The apical horn of this species lacks grooves. The wings of this species are solid cylindrical instead of latticed triangular. This species differs from *Pterocyrtidium genriettae* Nishimura (1992, pl. 8, figs. 11, 12, pl. 13, fig. 21) by having more closely spaced

pores and more prominent ribs between adjacent longitudinal rows of pores.

Occurrence.—Upper Paleocene in Tibet (Liang *et al.*, 2012).

Acknowledgments

We sincerely thank Christopher Hollis, an anonymous reviewer, and the editor Yasunari Shigeta for carefully and critically reviewing our paper. This study was financially supported by the National Natural Science Foundation of China Grant Number 41572188 and the Project of Geological Survey of China Grant Number 1212011086037. This study was financially supported in part by the Japan Society for the Promotion of Science KAKENHI Grant Numbers 15K05329 and 15H02142E. We sincerely thank Li Xiaohan and Zhang Xiaolong (China University of Geosciences, Beijing) for their cooperation in the field work.

References

- Aitchison, J. C., Ali, J. R. and Davis, A. M., 2007: When and where did India and Asia collide? *Journal of Geophysical Research, Solid Earth*, vol. 112, B05423, doi:10.1029/2006JB004706.
- Aitchison, J. C. and Davis, A. M., 2004: Evidence for the multiphase nature of the India–Asia collision from the Yarlung Tsangpo suture zone, Tibet. *Geological Society of London, Special Publications*, vol. 226, p. 217–233.
- Aitchison, J. C., Davis, A. M., Liu, J., Luo, H., Malpas, J. G., McDermid, I. R., Wu, H. Y., Zhiabrev, S. U. and Zhou, M. F., 2000: Remnants of a Cretaceous intra-oceanic subduction system within the Yarlung–Zangbo suture (southern Tibet). *Earth and Planetary Science Letters*, vol. 183, p. 231–244.
- Agnini, C., Fornaciari, E., Raffi, I., Rio, D., Röhl, U. and Westerhold, T., 2007: High-resolution nannofossil biochronology of middle Paleocene to early Eocene at ODP Site 1262: implications for calcareous nannoplankton evolution. *Marine Micropaleontology*, vol. 64, p. 215–248.
- Ali, J. R. and Aitchison, J. C., 2008: Gondwana to Asia: plate tectonics, paleogeography and the biological connectivity of the Indian subcontinent from the Middle Jurassic through latest Eocene (166–35 Ma). *Earth-Science Reviews*, vol. 88, p. 145–166.
- Beck, R. A., Burbank, D. W., Sercombe, W. J., Riley, G. W., Barndt, J. K., Rerry, J. R., Afzal, J., Khan, A. M., Jurgens, H., Metje, J., Cheema, A., Shafique, N. A., Lawrence, R. D. and Khan, M. A., 1995: Stratigraphic evidence for an early collision between north-west India and Asia. *Nature*, vol. 373, p. 55–58.
- Blome, C. D., 1992: Radiolarians from Leg 122, Exmouth and Wombat Plateaus, Indian Ocean, In, Rad, U. von *et al.*, *Proceedings of the Ocean Drilling Program, Scientific Results*, vol. 122, p. 633–652. Ocean Drilling Program, College Station.
- Borisenko, N. N., 1958: Paleocene Radiolaria of Western Kuban. In, Krylov, A. P. ed., *Voprosy geologii, bureniya i ekspluatatsii skvashin (Problems in geology, drilling and exploitation of wells). Trudy Vsesoyuznyi Neftegazovyi Nauchno-Issledovatel'skii Institut (VNI), Krasnodarskii Filial*, no. 17, p. 81–100. (in Russian; original title translated)
- Bustillo, M. A., Nishimura, A., Araña, V. and Hattori, I., 1994: Paleocene radiolarians from xenoliths hosted in Holocene lavas of Lanzarote (Canary Islands). *Geobios*, vol. 27, p. 181–188.
- Bütschli, O., 1882: Beiträge zur Kenntnis der Radiolarienskelette, insbesondere der Cyrtida. *Zeitschrift für Wissenschaftliche Zoologie*, vol. 36, p. 485–540.
- Campbell, A. S., 1954: Radiolaria. In, Moore, R. C. ed., *Treatise on Invertebrate Paleontology, Part D, Protista 3*, p. D11–D195. Geological Society of America, New York and University of Kansas Press, Lawrence.
- Clark, B. L. and Campbell, A. S., 1942: Eocene radiolarian faunas from the Monte Diablo area, California. *Geological Society of America, Special Paper*, no. 39, p. 1–106.
- Cluzel, D., Aitchison, J. C. and Picard, C., 2001: Tectonic accretion and underplating of mafic terranes in the Late Eocene intraoceanic fore-arc of New Caledonia (Southwest Pacific): geodynamic implications. *Tectonophysics*, vol. 340, p. 23–59.
- Coulon, C., Maluski, H., Bollinger, C. and Wang, S., 1986: Mesozoic and Cenozoic volcanic rocks from central and southern Tibet: ³⁹Ar–⁴⁰Ar dating, petrological characteristics and geodynamical significance. *Earth and Planetary Science Letters*, vol. 79, p. 281–302.
- Debon, F., Le Fort, P., Sheppard, S. M. and Sonet, J., 1986: The four plutonic belts of the Transhimalaya–Himalaya: A chemical, mineralogical, isotopic, and chronological synthesis along a Tibet–Nepal section. *Journal of Petrology*, vol. 27, p. 219–250.
- Ding, L., 2003: Paleocene deep-water sediments and radiolarian faunas: Implications for evolution of Yarlung–Zangbo foreland basin, southern Tibet. *Science in China Series D*, vol. 46, p. 503–515.
- Du, X. J., Chen, X., Wang, C. S., Wei, Y. S., Li, Y. L. and Jansa, L., 2015: Geochemistry and detrital zircon U–Pb dating of Lower Cretaceous volcanoclastics in the Babazhadong section, Northern Tethyan Himalaya: Implications for the breakup of Eastern Gondwana. *Cretaceous Research*, vol. 52, p. 127–137.
- Dumitrica, P., 1973: Paleocene Radiolaria, DSDP Leg 21. In, Burns, R. E., Andrews, J. E. *et al.*, *Initial Reports of the Deep Sea Drilling Project*, vol. 21, p. 787–817. U. S. Government Printing Office, Washington, DC.
- Ehrenberg, C. G., 1838: Über die Bildung der Kreidefelsen und des Kreidemergels durch unsichtbare Organismen. *Abhandlungen der Königl. Akademie der Wissenschaften zu Berlin*, Jahre 1838, p. 59–147.
- Ehrenberg, C. G., 1847: Über eine halibolithische, von Herrn R. Schomburgk entdeckte, vorherrschend aus mikroskopischen Polycystinen gebildete, Gebirgsmasse von Barbados. *Monatsbericht Königl. Preussischen Akademie der Wissenschaften zu Berlin*, Jahre 1846, p. 382–385.
- Ehrenberg, C. G., 1854: *Mikrogeologie. Das Erden und Felsen schaffende Wirken des unsichtbar kleinen selbstständigen Lebens auf der Erde*, xxviii + 374 p., Atlas, 31 p. Leopold Voss, Leipzig.
- Ehrenberg, C. G., 1873: Grossere Felsproben des Polycystinen-Mergels von Barbados mit weiteren Erläuterungen. *Königliche Preussische Akademie der Wissenschaften zu Berlin, Monatsberichte*, Jahre 1873, p. 213–263.
- Ehrenberg, C. G., 1875: Fortsetzung der mikrogeologischen Studien als Gesamt-Übersicht der mikroskopischen Paläontologie gleichartig analysirter Gebirgsarten der Erde, mit specieller Rücksicht auf den Polycystinen-Mergel von Barbados. *Abhandlungen Königl. Akademie der Wissenschaften zu Berlin*, Jahre 1875, p. 1–225.
- Einsele, G., Liu, B., Dürr, S., Frisch, W., Liu, G., Luterbacher, H. P., Ratschbacher, L., Ricken, W., Wendt, J., Wetzel, A., Yu, G. and Zheng, H., 1994: The Xigaze forearc basin: Evolution and facies architecture (Cretaceous, Tibet). *Sedimentary Geology*, vol. 90, p.

- 1–32.
- Foreman, H. P., 1973: Radiolaria of Leg 10 with systematics and ranges for the families Amphipyndacidae, Artostrobiidae and Theoperidae. In: Worzel, J. L., Bryant, W. *et al.*, *Initial Reports of the Deep Sea Drilling Project*, vol. 10, p. 407–474. U. S. Government Printing Office, Washington, DC.
- Frizzell, D. L. and Middour, E. S., 1951: Paleocene radiolaria from southeastern Missouri. *Bulletin University of Missouri School of Mines and Metallurgy, Technical Series*, vol. 77, p.1–41.
- Gradstein, F. M., Ogg, J. G., Schmitz, M. D. and Ogg, G. M. *eds.*, 2012: *The Geological Time Scale 2012*, 1144 p. Elsevier, Amsterdam.
- Haeckel, E., 1881: Entwurf eines Radiolarien-Systems auf Grund von Studien der Challenger-Radiolarien. *Jenaische Zeitschrift für Naturwissenschaft*, vol. 15, p. 418–472.
- Haeckel, E., 1887: Report on the Radiolaria collected by H.M.S. Challenger during the years 1873–1876. *Report on the Scientific Results of the Voyage of the H.M.S. Challenger, Zoology*, vol. 18, p. 1–1803.
- Hollis, C. J., 1993: Latest Cretaceous to Late Paleocene radiolarian biostratigraphy: A new zonation from the New Zealand region. *Marine Micropaleontology*, vol. 21, p. 295–327.
- Hollis, C. J., 1997: Cretaceous–Paleocene Radiolaria from eastern Marlborough, New Zealand. *Institute of Geological and Nuclear Sciences Monograph*, vol. 17, p. 1–152.
- Hollis, C. J., 2002: Biostratigraphy and paleoceanographic significance of Paleocene radiolarians from offshore eastern New Zealand. *Marine Micropaleontology*, vol. 46, p. 265–316.
- Hollis, C. J., 2006: Radiolarian faunal turnover through the Paleocene–Eocene transition, Mead Stream, New Zealand. *Eclogae Geologicae Helvetiae*, vol. 99, supplement 1, p. 79–99.
- Hollis, C. J. and Hanson, J. A., 1991: Well-preserved Late Paleocene Radiolaria from Tangihua Complex, Camp Bay, eastern Northland. *Tane*, vol. 33, p. 65–76.
- Hu, X. M., Garzanti, E., Moore, T. and Raffi, I., 2015: Direct stratigraphic dating of India–Asia collision onset at the Selandian (middle Paleocene, 59±1 Ma). *Geology*, vol. 43, p. 859–862.
- Hu, X. M., Jansa, L. and Wang, C. S., 2008: Upper Jurassic–Lower Cretaceous stratigraphy in south-eastern Tibet: a comparison with the western Himalayas. *Cretaceous Research*, vol. 29, p. 301–315.
- Hebei Institute of Geological Survey, 2005: 1:250000 Yagra, Burang, Horba and Babazhadong Sheets in Xizang. *Sedimentary Geology and Tethyan Geology*, vol. 33, p. 80–86. (in Chinese with English abstract)
- Jackett, S. J., Baumgartner, P. O. and Bandini, A. N., 2008: A new low-latitude late Paleocene–early Eocene radiolarian biozonation based on unitary associations: applications for accreted terranes. *Stratigraphy*, vol. 54, p. 39–62.
- Jannou, G., 2007: Radiolarios del Paleógeno de cuenca Austral, Tierra del Fuego, Argentina. *Ameghiniana*, vol. 44, p. 447–466.
- Kozlova, G. E., 1999: Paleogene Boreal Radiolarians from Russia. *Practical Manual of Microfauna of Russia*, vol. 9, p. 1–393. (in Russian with English title)
- Krashennnikov, V. A., 1960: Some radiolarians of the Lower and Middle Eocene of the Western Pre-Caucasus. *Trudy Vsesoyuznogo Nauchno-Issledovatel'skogo Geologorazvedochnogo Neftyanogo Instituta (Paleontologicheskii Sbornik 3)*, vyp. 16, p. 271–308.
- Li, X., Matsuoka, A., Li, Y. L. and Wang, C. S., 2017: Phyletic evolution of the mid-Cretaceous radiolarian genus *Turbocapsula* from southern Tibet and its applications in zonation. *Marine Micropaleontology*, vol. 130, p. 29–42.
- Li, X. H., Wang, C. S., Wan, X. Q. and Tao, R., 1999: Verification of stratigraphic sequence and classification for the Chuangde cross-locality of Gyangze, southern Tibet. *Journal of Stratigraphy*, vol. 23, p. 303–309. (in Chinese with English abstract)
- Li, Y. L., Wang, C. S., Hu, X. M., Bak, M., Wang, J. J. and Chen, L., 2007: Characteristics of Early Eocene radiolarian assemblages of the Saga area, southern Tibet and their constraint on the closure history of the Tethys. *Chinese Science Bulletin*, vol. 52, p. 2108–2114.
- Liang, Y. P., Zhang, K. X., Xu, Y. D., He, W. H., An, X. Y. and Yang, Y. F., 2012: Late Paleocene radiolarian fauna from Tibet and its geological implications. *Canadian Journal of Earth Sciences*, vol. 49, p. 1364–1371.
- Liu, J., Aitchison, J. C. and Ali, J. R., 2011: Upper Paleocene radiolarians from DSDP Sites 549 and 550, Goban Spur, NE Atlantic. *Palaeoworld*, vol. 20, p. 218–231.
- Liu, G. and Einsele, G., 1994: Sedimentary history of the Tethyan basin in the Tibetan Himalayas. *Geologische Rundschau*, vol. 83, p. 32–61.
- Liu, G. and Einsele, G., 1996: Various types of olistostromes in a closing ocean basin, Tethyan Himalaya (Cretaceous, Tibet). *Sedimentary Geology*, vol. 104, p. 203–226.
- Liu, J. B. and Aitchison, J. C., 2002: Upper Paleocene radiolarians from the Yamdrok mélange, south Xizang (Tibet), China. *Micropaleontology*, vol. 48, supplement 1, p. 145–154.
- Maluski, G., Proust, F. and Xiao, X. C., 1982: ³⁹Ar/⁴⁰Ar dating of the trans-Himalayan calc-alkaline magmatism of southern Tibet. *Nature*, vol. 298, p. 152–154.
- Najman, Y., 2006: The detrital record of orogenesis: A review of approaches and techniques used in the Himalayan sedimentary basins. *Earth-Science Reviews*, vol. 74, p. 1–72.
- Nanayama, F., 1992: Stratigraphy and facies of the Paleocene Nakanogawa Group in the southern part of central Hokkaido. *Journal of the Geological Society of Japan*, vol. 98, p. 1041–1059.
- Nicolas, A., Girardeau, J., Marcoux, J., Dupre, B., Wan, X., Cao, Y., Zheng, H. and Xiao, X., 1981: The Xigaze ophiolite (Tibet): a peculiar oceanic lithosphere. *Nature*, vol. 294, p. 414–417.
- Nishimura, A., 1987: Cenozoic Radiolaria in the western North Atlantic, Site 603, Leg 93 of the Deep Sea Drilling Project. In: Van Hinte, J. E. *et al.*, *Initial Reports of the Deep Sea Drilling Project*, vol. 93, p. 713–737. U. S. Government Printing Office, Washington, DC.
- Nishimura, A., 1992: Paleocene radiolarian biostratigraphy in the northwest Atlantic at Site 384, Leg 43, of the Deep Sea Drilling Project. *Micropaleontology*, vol. 38, p. 317–362.
- Nishimura, A., 2001: Paleocene Radiolarians from DSDP Leg 43, Site 384 in the Northwest Atlantic. *News of Osaka Micropaleontologists, Special Volume*, no. 12, p. 293–320.
- Norris, R. D., Wilson, P. A., Blum, P. and the Expedition 342 Scientists, 2014: Methods. In: Norris, R. D., Wilson, P. A., Blum, P. and the Expedition 342 Scientists, *Proceedings of the Integrated Ocean Drilling Program*, vol. 342, p. 1–78. Integrated Ocean Drilling Program, College Station.
- O'Connor, B., 2001: *Buryella* (Radiolaria, Artostrobiidae) from DSDP site 208 and ODP site 1121. *Micropaleontology*, vol. 47, p. 1–22.
- O'Dogherty, L., 1994: Biochronology and paleontology of Mid-Cretaceous radiolarians from Northern Apennines (Italy) and Betic Cordillera (Spain). *Mémoires de Géologie (Lausanne)*, no. 21, p. 1–415.
- Okada, H. and Bukry, D., 1980: Supplementary modification and introduction of code numbers to the low-latitude coccolith biostratigraphic zonation. *Marine Micropaleontology*, vol. 5, p. 321–325.
- Oyaizu, A., Miura, K., Tanaka, T., Hayashi, H. and Kiminami, K., 2002: Geology and radiolarian ages of the Shimanto Supergroup, western Shikoku, Southwest Japan. *Journal of the Geological Society of Japan*, vol. 108, p. 701–720.

- Petrushevskaya, M. G., 1975: Cenozoic radiolarians of the Antarctic, Leg 29, DSDP. *In*, Kennett, J. P. *ed.*, *Initial Reports of the Deep Sea Drilling Project*, vol. 29, p. 541–675. U. S. Government Printing Office, Washington, DC.
- Petrushevskaya, M. G. and Kozlova, G. E., 1972: Radiolaria: Leg 14, Deep Sea Drilling Project. *In*, Hayes, D. E. and Pimm, A. C., *eds.*, *Initial Reports of the Deep Sea Drilling Project*, vol. 14, p. 495–648. U. S. Government Printing Office, Washington, DC.
- Riedel, W. R., 1967: Subclass Radiolaria. *In*, Harland, W. B. *et al.*, *eds.*, *The Fossil Record*, p. 291–298. Geological Society of London, London.
- Riedel, W. R. and Sanfilippo, A., 1971: Cenozoic Radiolaria from the western tropical Pacific, Leg 7. *In*, Winterer, E. L. *et al.*, *Initial Reports of the Deep Sea Drilling Project*, vol. 7, p. 1529–1672. U. S. Government Printing Office, Washington, DC.
- Riedel, W. R. and Sanfilippo, A., 1973: Cenozoic Radiolaria from the Caribbean, Deep Sea Drilling Project, Leg 15. *In*, Edgar, N. T. and Saunders, J. B. *eds.*, *Initial Reports of the Deep Sea Drilling Project*, vol. 15, p. 705–751. U. S. Government Printing Office, Washington, DC.
- Sanfilippo, A. and Blome, C. D., 2001: Biostratigraphic implications of mid-latitude Paleocene–Eocene radiolarian faunas from Hole 1051A, Ocean Drilling Program Leg 171B, Blake Nose, western North Atlantic. *In*, Kroon, D., Norris, R. D. and Klaus, A. *eds.*, *Western North Atlantic Palaeogene and Cretaceous Palaeoceanography*, vol. 183, p. 185–224. Geological Society of London Special Publication.
- Sanfilippo, A., Hakyemez, A. and Tekin, U. K., 2003: Biostratigraphy of Late Paleocene–Middle Eocene radiolarians and foraminifera from Cyprus. *Micropaleontology*, vol. 49, p. 47–64.
- Sanfilippo, A., Hull, D. M. and Flores-Abin, E., 1999: Upper Paleocene–lower Eocene radiolarian biostratigraphy of the San Francisco de Paula section, western Cuba: Regional and global comparisons. *Micropaleontology*, vol. 45, supplement 2, p. 57–82.
- Sanfilippo, A. and Nigrini, C., 1998a: Upper Paleocene–Lower Eocene deep-sea radiolarian stratigraphy and the Paleocene/Eocene Series boundary. *In*, Aubry, M.-P. *et al.*, *Late Paleocene–Early Eocene climatic and biotic events in the marine and terrestrial records*, p. 244–276. Columbia University Press, New York.
- Sanfilippo, A. and Nigrini, C., 1998b: Code numbers for Cenozoic low latitude radiolarian biostratigraphic zones and GPTS conversion tables. *Marine Micropaleontology*, vol. 33, p. 109–156.
- Sanfilippo, A. and Riedel, W. R., 1973: Cenozoic Radiolaria (exclusive of theoperids, artostrobiids and amphipyndacids) from the Gulf of Mexico, DSDP Leg 10. *In*, Worzel, J. L., Bryant, W. *et al.*, *Initial Reports of the Deep Sea Drilling Project*, vol. 10, p. 475–611. U. S. Government Printing Office, Washington, DC.
- Strong, C. P., Hollis, C. J. and Wilson, G. J., 1995: Foraminiferal, radiolarian, and dinoflagellate biostratigraphy of Late Cretaceous to Middle Eocene pelagic sediments (Muzzle group), Mead Stream, Marlborough, New Zealand. *New Zealand Journal of Geology and Geophysics*, vol. 38, p. 171–209.
- Wade, B. S., Pearson, P. N., Berggren, W. A. and Pälike, H., 2011: Review and revision of Cenozoic tropical planktonic foraminiferal biostratigraphy and calibration to the geomagnetic polarity and astronomical time scale. *Earth-Science Reviews*, vol. 104, p. 111–142.
- Wan, X., Zhao, W. and Li, G., 2000: Restudy of the Upper Cretaceous in Gamba, Tibet. *Geoscience*, vol. 14, p. 281–285.
- Wang, C. S., Li, X., Wan, X. and Tao, R., 2000: The Cretaceous in Gyangze, southern Tibet. *Acta Geologica Sinica*, vol. 74, p. 97–107. (*in Chinese with English abstract*)
- Wen, S., 1987: Tertiary system. *In*, Xizang Scientific Expedition, Chinese Academy of Sciences *eds.*, *Stratigraphy of the Mount Qomolangma Region*, p. 130–159. Science Press, Beijing. (*in Chinese with English title*)
- Willems, H., Zhou, Z., Zhang, B. and Grafe, K. U., 1996: Stratigraphy of the Upper Cretaceous and Lower Tertiary strata in the Tethyan Himalayas of Tibet (Tingri area, China). *Geologische Rundschau*, vol. 85, p. 723–754.
- Xu, Y., 2000: Early Tertiary calcareous nannofossils from southern Tibet and the closing time of east Tethys in Tibet. *Geoscience*, vol. 14, p. 255–262.
- Yin, A. and Harrison, T. M., 2000: Geologic evolution of the Himalayan–Tibetan orogen. *Annual Review of Earth and Planetary Sciences*, vol. 28, p. 211–280.
- Zhou, Y. Z., Fu, W., Yang, Z. J., Nie, F. J., He, J. G., Zhao, Y. Y., Li, Z. Q., Shi, G. Y. and Li, W., 2007: Microfabrics of chert from Yarlung Zangbo Suture Zone and southern Tibet and its geological implications. *Acta Petrologica Sinica*, vol. 22, p. 742–750. (*in Chinese with English abstract*)